REVIEW PAPER
"RESPONSE OF WIDE SPAN ENCLOSURES TO WIND ACTION"

G. Bartoli, R. Bertero, N. Blaise, N. Cosentino, V. Denoël, G. Diana, M. Majowiecki (coordinator), A. Zasso

1 INTRODUCTION

Wide span enclosures usually deal with structural typologies as space structures, cable structures, membrane structures and new efficient materials. This paper contains historical review of theoretical and experimental progresses in the evaluation of the response of the wide span enclosures to wind action. Theoretical and experimental in scale analyses combined with a monitoring control of the subsequent performance of the structural system, can calibrate mathematical modeling and evaluate structures aerodynamic and aeroelastic behaviour and long term reliability of the design. Large dimensions and lightweight structure behaviour is difficult to identify and no help is provided in this direction by either literature or standard codes. Due to the variety of geometries and sites, general provisions of the codes could not cover all the situations and generally they address only small-medium scale projects. In these cases, deeper studies, using analytical, computational and model test methods, can be very helpful, since they allow to account for the specific geometry, surroundings and local climatic factors. Different standard codes usually allow these types of studies through their "equivalency" clause and various references to special studies.

In the second half of 80s, the response of sub-horizontal wide span enclosures to wind action started to be investigated and the main problems - still largely present - were outlined [1]; experimental investigation on scale model gave the possibility of first comparative analyses. Before these experiences, the loads distribution on upper and lower surfaces and the probability density function distribution for large span roofs and canopies were not investigated.

These aspects were firstly faced during the design of football stadia for "Italia 90" World Cup and scientific and experimental studies were carried out at the Western Ontario Boundary Layer Wind Tunnel (BLWT). Wind loading-experimental analyses on scale models were led on a rigid model of the "Stadio delle Alpi" in Turin, and for a flexible model of the Olympic Stadium in Rome. Moreover, a new very practical method to obtain the structural response under the random wind action and small displacement (linear response) was applied; this procedure (based on "orthogonal decomposition method") led to simplify the use of the large amount of recorded signals (local pressure time histories) from which the model load cases could be constructed and the analyses conducted in either the time or frequency domain.

Experimental analyses carried out on rigid models allowed to measure maximum values of the pressure coefficient to obtain the net load on each panel. Due to a non-Gaussian trend of the load, many errors on the fluctuating part of the theoretical response on common period were identified. Moreover theoretical analyses compared with experimental ones, showed that: the spectra obtained from the two different analyses present very distant responses; the pressure coefficients could not be independent of time; the aerodynamic stiffness and damping are necessary to simulate the actual behavior of the structure in the analyses.

At that time, very limited experimental possibilities were allowable to evaluate the correlation, as few pressure taps could be used simultaneously. On the other side, once the problem of simultaneous acquisitions of taps was solved, the problem of dealing the large volume of data in an engineering and effective way occurred.

The two main tasks of wind tunnel testing on large span roofs were addressed: (i) to the wind tunnel model setup; (ii) to the presentation of experimental data to the designer in a suitable way to be used in the numerical models. Wind tunnel investigation of the behavior of wind on the cable supported roof of the "Stadio delle Alpi" in Turin [2] allowed to get local and area-averaged pressures on the roof and the motions observed on a 1:200 model. Notice that the major part of the loading is dynamic in nature and is due to vortices produced in the wake of the upstream sector of the roof and producing vertical velocity fluctuations in the flow approaching the leading edge of the downstream sector. The study of the Turin and Rome stadia drew attention on the inability of the measuring system employed to provide data in a form that could be used readily as input to the sophisticated dynamic numerical model developed by the designer and lead to discussions between the designer and the wind tunnel researches to examine alternative techniques that might be used in future projects. Improved experimental techniques, involving a multi-point high speed pressure scanning system and a suitable set of load pattern time histories, allowed to overcome a part of these difficulties, producing a complete description of the load.

Within the framework of wind engineering problems, it is widely established that to obtain realistic results from model tests, it is necessary to accurately model both the object being studied and the characteristics of the oncoming wind. In particular every complete modeling of suspension systems as well as lightweight roof systems involves an accurate fluid-structure analysis. Both the modeling of wind flows over the structure and the mechanical model of the structure itself, within the framework of geometrically nonlinear field, must be introduced, by considering aeroelastic interaction. The pressure field, by considering the effect of vortex shedding, as well as the pressure coefficients has to be evaluated.

Uncertainties related to random distribution of live load on long span structures imply very careful loading analyses combined with specific experimental tests; investigations about actual live load distribution and intensity on large covering surfaces are therefore necessary to identify the actual behaviour of the structure. Snow drift and accumulation factors (in addition to dynamic action to wind loading) represent one of the most important experimental investigation about live load distribution in designing large coverings [3]. Specific analyses have been carried out on a scale model of the Montreal Olympic Stadium to predict a possible failure resulting from patchy accumulations of snow on the roof. The actual phenomenon is related to the snow-wind loads combination, because the anomalous accumulation is due to the separation of the air flow and turbulence in the wake. The drastic reduction in the ratio of permanent weight to variable load makes lightweight structures particularly sensitive to the effects of wind and snow. The dynamic nature of wind action can cause oscillations and deformations of such amplitude that they jeopardise the function of the roof and, in the worst cases, its structural stability. On the other hand, the static effect of snow represents an extremely heavy load for this type of structure, even reaching as much as 70-80% of the total load. Melchers [4] demonstrated that one of the primary causes of collapse (corresponding to approximately 45% of the cases analysed) lies in an erroneous evaluation of the loading conditions and of the structural response. With improvements in the methods for in-depth analysis in the design of lightweight wide-span roofing, theoretical studies can and must be used in combination with experimental tests performed in wind tunnels and in situ. From the observation of structures that have completely or partially collapsed: (i) due to snow, e.g. the Hartford Coliseum (1978), the Pontiac Stadium (1982), the Milan Sports Hall (1985) and the Montreal Olympic Stadium (1992); (ii) due to wind, e.g. the Montreal Olympic Stadium (1988); (iii) due to the effects of water, e.g. the Minnesota Metrodome (1983).

Considering the statistical results of Majowiecki [5], and the "scale effect" of long span structures several special design aspects arose as: (i) the snow distribution and accumulations on large covering areas in function of statistically correlated wind direction and intensity; (ii) the wind pressure distribution on large areas considering theoretical and experimental correlated power

spectral densities or time histories; (iii) rigid and aeroelastic response of large structures under the action of cross-correlated random wind action considering static, quasi-static and resonant contributions; (iv) the time dependent effect of coactive indirect actions as pre-stressing, short and long term creeping and temperature effects; (v) the local and global structural instability; (vi) the nonlinear geometric and material behaviour; (vii) reliability and safety factors of new hi-tech composite materials; (viii) the necessity to avoid and short-circuit progressive collapse of the structural system due to local secondary structural element and detail accidental failure; (ix) the compatibility of internal and external restraints and detail design, with the modeling hypothesis and real structural system response; (x) the parametric sensibility of the structural system depending on the type and degree of static indeterminacy and hybrid collaboration between hardening and softening behaviour of substructures.

Knowledge based and conceptual design plays an essential role in removing gross human intervention errors from initial design statements. Moreover design assisted by experimental investigation is a useful integration of the design process of wide span structures.

The following two sections will describe, respectively, the "physical aspects of wind on wide span structures" and "standard codes, testing and numerical tools".
In particular, section 2 will describe the physical phenomena to be considered in the design of wide span enclosures and the evaluation of their response to wind action, with reference to real examples. The attention will be focused on: basic aerodynamic effects, above all, vortex shedding, peak pressures and limits of quasi-steady approach; aeroelastic effects on roof surface and on supporting cables (end-support motion and support-structure interaction); physical meaning and effects of aerodynamic stiffness and aerodynamic damping; additional tasks are considered in closed or semi-closed spaces; wind-snow interaction effects.
Section 3 will focus on analytical and numerical tools to study wide span enclosures subjected to wind action; state of the art and "open problems" will be reported, as well as contents of standard codes and limits in their application for complex geometries; scale effects, morphology and problems for free form structures.

2 WIND ON WIDE SPAN STRUCTURES - PHYSICAL ASPECTS

2.1 Aerodynamic Effects: Mean, Quasi-Steady and Resonant Contributions; Vortex Shedding

The first systematic approach to the design assisted by wind tunnel testing began in the early '90s. Since these initial tests [2], it was shown that the vortex shedding was the main source of aerodynamic excitation. Moreover, it was demonstrated that significant values of the pressure coefficients oscillate around mean values close to zero.

Load as a function of wind direction was investigated by Vickery and Majowiecki through experimental tests on both a rigid and an aeroelastic model of the Turin Stadium (Fig.1): rigid model tests were oriented to measure pressure at upper and lower roof faces; an aeroelastic model was designed to match the Froude number. Local point pressure in a rigid model was investigated using sixteen transducers to measure net load (upper-lower surface load) on eight panels and the corresponding power spectral density matrix is provided. The measurements on the aeroelastic model were limited to the deflection on five locations and to the tensions in two of the back-stays. Investigation of loads and deflection was complicated by the inability of the instrumentation system to provide a complete description of the model; for this reason correlation between pressure in various points of the roof was not simple to obtain and correlation between different magnitudes could not be extended to the whole field of study.

The inability of the instrumentation system to provide a complete description of the loading also occurred during tests on the model of Turin Stadium, only seven out of about sixty panels were instrumented and the data obtained were interpolated to provide estimates of the overall loading; the interpolation required is concerned not only with the magnitude of the panel loads but also the spectra and cross-spectra. Noting that linear interpolation in time or space, as used at that time, was shown to be inaccurate (see ref. [6]).

Load was presented in a coefficient form expressed as:

$$C_p=(P_u-P_L)/\frac{1}{2}\rho V_R^2\cdot A \qquad (1)$$

where: P_u is the load on upper surface, P_L the load on lower surface, A the panel area and V_R the mean speed at a height of 30 m in the approach flow. Selected panel loads, maximum, minimum and mean values of load was plotted as a function of wind direction, as shown in Fig.1.

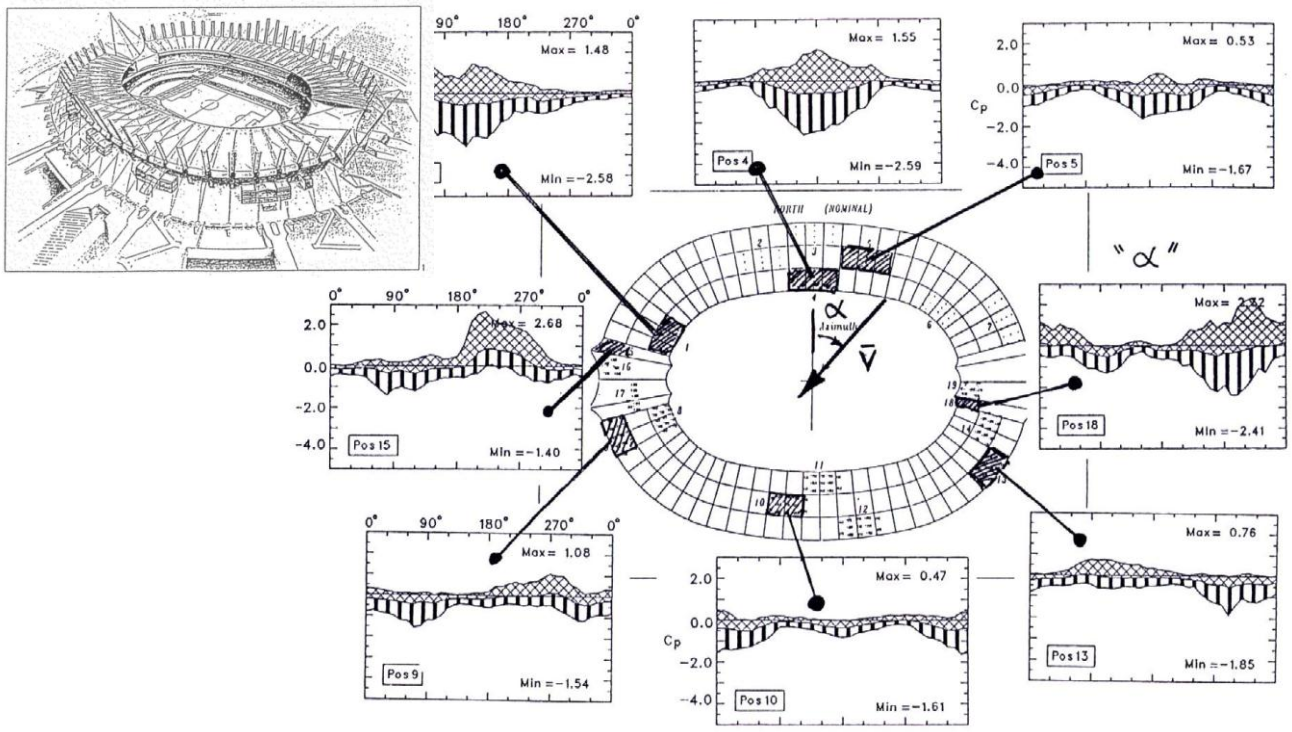

Fig.1 "Stadio delle Alpi, Turin: general view and panel load as a function of wind direction, from [2], 1992

Diagrams in Fig.1 show that:

(i) the mean pressure coefficients are generally small with maximum values of about 0.5;
(ii) the dynamic component is dominant and the peak load for the more important cases is five times the mean;
(iii) leading edge panels are the most heavily loaded and, very roughly, the load is proportional to the cosine of the angle between the wind and the normal to the leading edge.

A comparative analysis between experimental investigation on scale model of Rome and Turin Stadia and a theoretical model for the random dynamical analysis of large quasi-horizontal

coverings was carried out by Majowiecki [7]. The theoretical model appeared to be not completely consistent. The description of pressure distribution on covering surface cannot disregard the transversal component of the wind and also is impossible to give the vectorial role to pressure coefficients C_p, independent of time, to change the direction from along wind to normal pressure distribution.

The quasi-steady theory [8] considers two terms of wind load to describe the wind action: the mean value and the fluctuating one. According to the experience reported in [7], this theory does not mirror wind effects, so that it could not be employed to compare results from tests and theory. In defining the structural load cases, local peak loading is not simultaneously acting over the roof, because the roof shape induces separations of the air flow and turbulence, so that the values of pressure coefficients are similar in up-lift or down-lift conditions as shown in Fig.1.

In substance, the integration of the wind tunnel data into the design process presents significant problems for wide span sub-horizontal enclosures; in contrast to buildings (high rise buildings) where knowledge of the base moment provides a sound basis for preliminary design, there is no single simple measure a the roof structure. The study of the Turin and Rome stadia [2]-[9]-[10] drew attention to the inability of the measuring system employed to provide data in a form that could readily be based as input to the sophisticated dynamic numerical model developed by the designer and lead to the discussion between the designer and the wind tunnel researchers to examine alternative techniques that might be used in future projects. Recent works on the envelope reconstruction problem [77] seem to throw light on some promising methods.

The analysis of auto and cross-spectra density functions showed that the vortices shed from one side of the roof could exciting the opposite side, as illustrated by Vickery and Majowiecki [2]. Typical spectra of panel load are presented in Fig.2; of note is the tendency for panels 3 and 4 to have a peak for a wind load investing roof with an angle of 180°. This peak can be attributed to vertical velocity fluctuations produced by vortices from the upstream sector of the stadium. In other words, the wind-structure interaction changes the "structure" of the wind flow and, due to the large dimensions, the downstream region of the roof "feels" the modified velocity field.

The Strouhal number (S_t), corresponding to the abscissa of the peak of the power spectrum, is:

$$St = f_s h / \bar{u}(h) \cong 0.12 \qquad (2)$$

where f_s is the central shedding frequency, h the roof height above upstream ground and u(h) the mean stream at this height.

The value of S_t is strongly related to the value of h, the size of the object invested by wind action: vortex shedding is therefore related to this parameter.

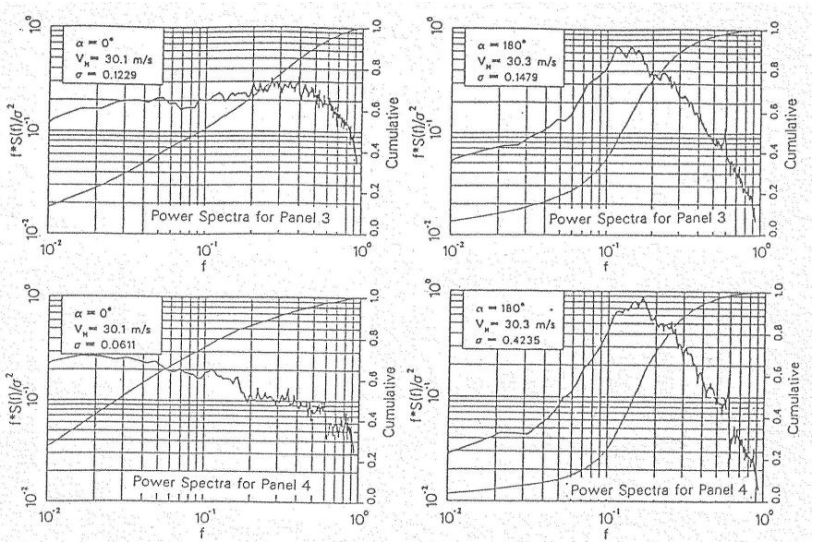

Fig.2 Typical spectra of the panel load, [2], 1992

In the examined case, the lowest natural frequency of the roof is about 0.6 Hz and sufficiently away from the vortex shedding frequency to avoid excessive resonant response. The cross-spectra density matrix gives the correlation of panel loads as shown in Fig.3. Of note is the very weak correlation (root coherence), even between nearly adjacent panels, at the natural frequency. Near the shedding frequency the correlation is strong (typically 80%) over the most heavily loaded section of the roof, like the central section containing 2, 3, 4 and 5. Hence, the vortex shedding can be considered as a local phenomenon, independent from the global behavior.

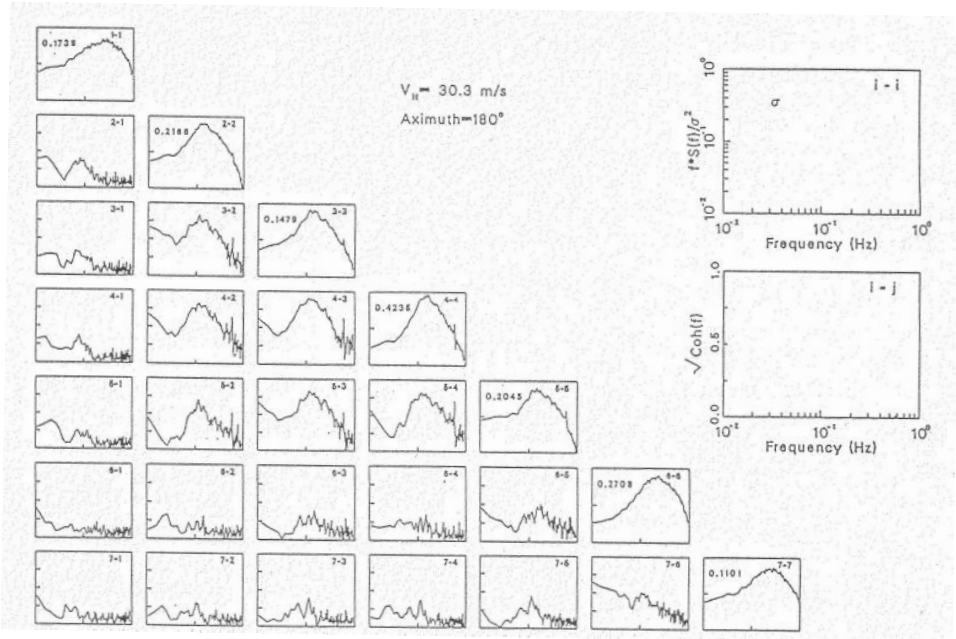

Fig.3 Auto-spectra and root-coherence functions of panel loads for a reference speed of 30 m/s and a wind angle of 180°

The results from aeroelastic tests are shown in Figs. 4 and 5. Fig. 4 shows the roof deflections as a function of wind direction, while typical spectra are presented in Fig. 5. The deflections mirror the panel loads with small mean values and large dynamic motions when the wind is normal to the leading edge of the roof. For the largest deflections, eg. location 4 at 180°, the bulk of variance is associated with shedding with a comparatively minor contribution due to resonance at the natural

frequency.

The resonant response is far more significant (relative to the total variance) on the upstream section of the roof (eg. location 3 and 5 at 180°) but is nevertheless much smaller than the vortex force motions when the segment is on the downstream part of the roof. As a matter of fact, down-stream part is directly excited by the vortex shedding, while up-stream part (and the whole roof) results indirectly excited through the involved modal shape.

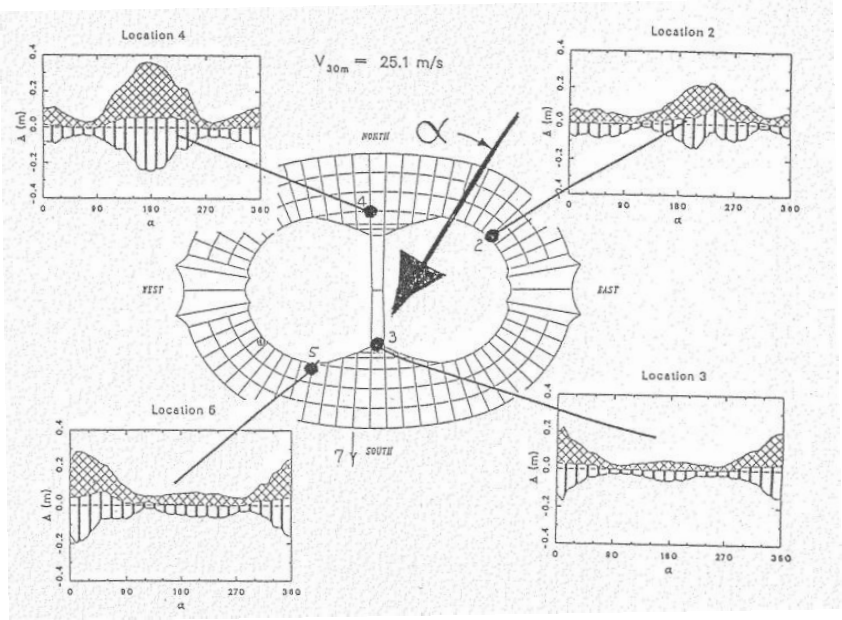

Fig.4 Roof deflections as a function of wind angle

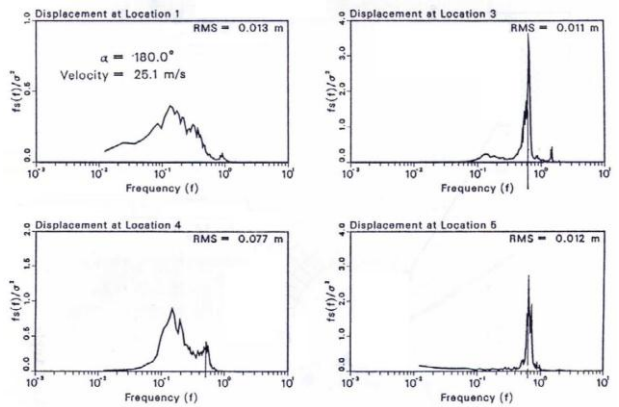

Fig.5 Selected spectra of roof deflection

The undisturbed wind velocities, as well as the forces/pressures on normal-to-wind surfaces, are usually assumed to be "Gaussian" in the technical literature. In the case of sub-horizontal surfaces, such as in wide span roofs, experimental data showed that the gust factors (Fig. 6) range from 3.9 to 6.9, so that the statistical load description is far from the gaussianity assumptions. Subsequently, the

common theoretical procedures can lead to important errors in evaluating the fluctuating part of the response, especially for its background component except if advanced analytical tools are considered [11].

Pressure Coefficients

PANEL	UPPER SURFACE max	min	mean	rms	LOWER SURFACE max	min	mean	rms	FULL PANEL NET max	min	mean	rms	g
1	0.14	-0.80	-0.30	0.10	0.29	-0.31	0.03	0.06	0.19	-0.80	-0.27	0.10	4.6
2	0.40	-1.10	-0.37	0.18	0.93	-0.43	0.08	0.14	1.23	-1.22	-0.30	0.24	6.4
3	0.28	-0.83	-0.31	0.12	0.40	-0.35	0.04	0.09	0.29	-0.91	-0.28	0.13	4.4
4	0.50	-1.19	-0.37	0.17	0.88	-0.40	0.08	0.14	1.29	-1.26	-0.29	0.23	6.9
5	0.20	-0.93	-0.36	0.12	0.47	-0.36	0.06	0.09	0.41	-0.99	-0.30	0.15	4.7
6	0.15	-0.77	-0.29	0.09	0.40	-0.24	0.10	0.07	0.26	-0.72	-0.20	0.10	4.6
7	0.24	-1.12	-0.40	0.14	0.67	-0.29	0.12	0.08	0.66	-1.02	-0.27	0.15	6.2
8	0.11	-0.58	-0.24	0.08	0.38	-0.17	0.12	0.06	0.16	-0.48	-0.11	0.07	3.9

a)

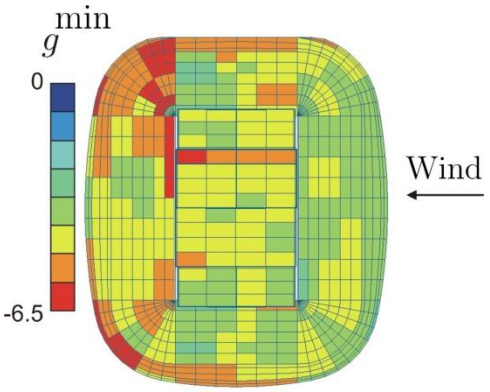

b)

Fig.6 Pressure coefficients and experimental gust- factors (azimuth = 0 deg) for Turin Stadium (a) and for Lille Stadium (b).

Unfortunately, the specific response depends on the shape roof and on the surrounding, so that general rules cannot be identified for the wind dynamic excitation due to the cited phenomena.

Based on some experiences, as for instance the Braga Stadium (Fig.7), experimental data [12;13] showed the pressure coefficients to be significantly lower – both in mean values and standard deviation – than those reported by standards (EC1) for similar geometry (such as canopies). Large values are essentially confined to the roof borders, corresponding to local vortex shedding. Hence, vortex induced pressures seem to not affect the global roof dynamics even if they can induce significant local stresses on the roof panels.

a)

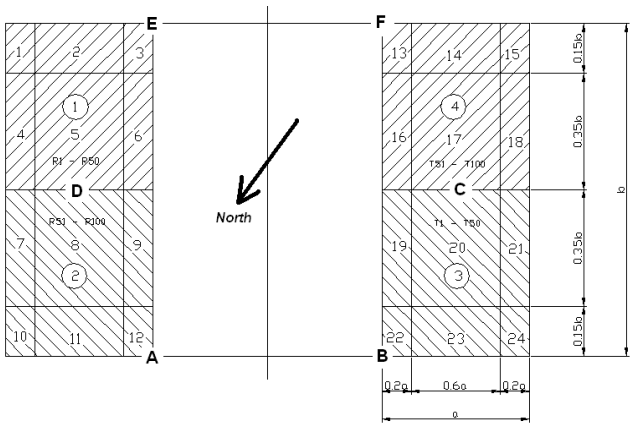

b)

Fig.7 a) View of the stadium from the south; b) scheme of the roof and location of significant measuring points (A-F)

The derived responses result is lower values than those derived by the standard (EC1) approach. Hence, the spatial uncorrelation effects should be greater than those approximately taken into account by the EC1 procedures.

To simplify the pressure representation and to reduce the computational effort, POD (proper orthogonal decomposition) technique was adopted. POD was introduced as an innovative method to express wind load and as approximate procedure to describe the effective action of the wind load on

structures; furthermore an appropriate use of this technique has proved to be very helpful to study the structural response with relatively simple analyses.

According to the simplified procedure suggested by Vickery [14-15-16], the structural response to wind action has been determined by separately evaluating (1) the mean response, (2) the quasi-steady response and (3) the resonant response. The first term takes into account the mean pressure distributions. The second one is obtained by performing a classical covariance proper orthogonal decomposition (POD). The third one takes into account the dynamic amplification of a suitable number of structural vibration modes, each of them being excited by the unsteady wind pressures.

A mixed approach of the analytical procedure was synthesized in the following equations and a typical result is summarized in Tab.1. The Equation 3 represents the procedure to decompose (POD) a pressure field (Fig.8), Equation 4 determines the mean and the quasi-steady response and Equation 5 displays the resonant contribution projected on the vibration modes of the structures.

$$C_p=\sum_{k=1}^{m}\phi_k\phi_k^T\lambda_k;\quad \phi_i\phi_j^T=\delta_{ij};\quad \phi_i^T C_p\phi_j=\delta_{ij}\lambda_j;\quad p(t)=\sum_{k=1}^{m}\phi_k\, x_k\,(t) \tag{3}$$

$$R(t)=\sum_{k=1}^{s}x_k\,(t)R_k;\quad \sigma_{R,qs}^2=\sum_{k=1}^{s}\sigma_{x_k}^2\,R_k^2;\quad R_{qs}=\overline{R}\pm g_{qs}\sigma_{R,qs} \tag{4}$$

$$\begin{gathered}R_{qs+\,res}=\overline{R}\pm\sqrt{g_{qs}{}^2\sigma_{R,qs}{}^2+g\ \ {}^2\sigma_{R,res}{}^2};\quad g\ \ {}^2\sigma_{R,res}{}^2=\sum_{h=1}^{n}g\ \ {}^2\sigma_{R_h}{}^2;\quad g_h=\sqrt{2\ln(f_hT)}+\frac{0.577}{\sqrt{2\ln(f_hT)}}\\ M_h=\int_A M(x,y)\psi_h^2(x,y)dA;\quad Q_h(t)=\int_A p(x,y,t)\psi_h(x,y)dA;\quad \sigma_{R_h}{}^2=R_h^2\frac{\pi}{4\xi_h}\frac{f_hS_{Q_h}(f_h)}{(2\pi f_h)^4M_h^2}\end{gathered} \tag{5}$$

As it will be better shown in next sections, POD technique allows to simplify an unsteady multivariate pressure field by projecting it on the space generated by the eigenvectors of the covariance matrix of the original field. Two main advantages can be achieved by this technique. Firstly, the new fields (pressure modes) are mutually uncorrelated. Secondly, the energy content of the complete multivariate field is usually well represented by few components in the transformed space, allowing the representation of the effective pressure field by means of few pressure modes. A possible third advantage consists in the physical correlation between pressure modes and aerodynamic phenomena (such as incident wind turbulence, vortex shedding, etc.). As a matter of fact, since the covariance is fully representative of the correlation only for Gaussian random processes, the pressure modes are mutually uncorrelated only for Gaussian multivariate pressure fields. POD method can be usefully applied for global actions (were the non-gaussianity becomes negligible) but not for the evaluation local loads.

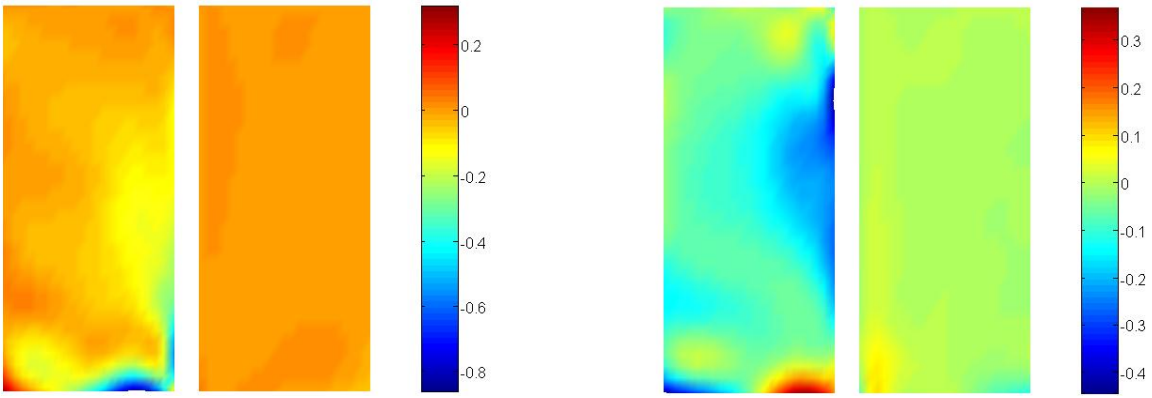

a) *b)*

Fig.8 Proper orthogonal decomposition of the measured wind pressure field: (a) Mode 1, σ^2=0.1449; (b) Mode 2, σ^2=0.0748

Pressure coefficient mean values and standard deviations, for a wind incidence of 270° from true north (the worst wind loading condition) according to the wind tunnel test on the Braga Stadium model are presented in Fig.9. The mean value is representative of generic mean response of the structure to wind actions, standard deviation and extreme values are representative of local fluctuation. Extreme values are confined in local zone, according to the previous observation that vortex shedding is a limited event.

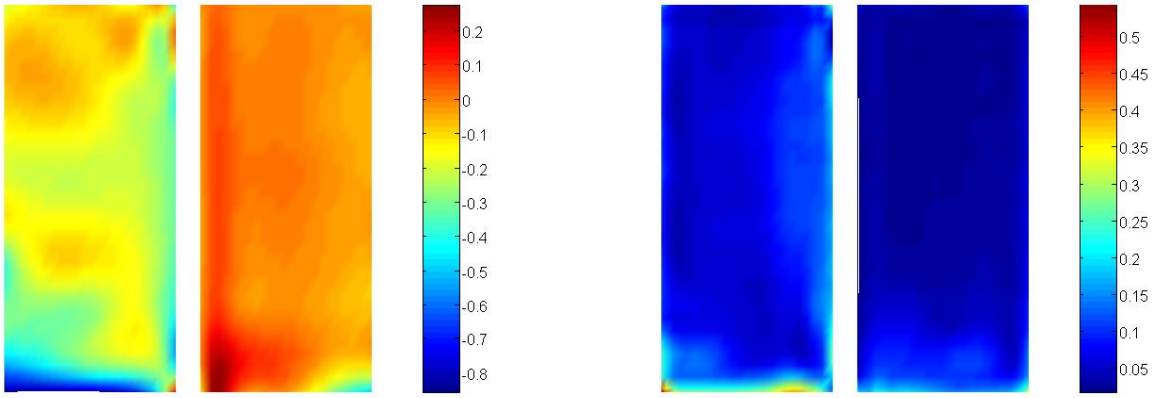

a) *b)*

Fig.9 Pressure coefficient: (a) mean values and (b) standard deviations for wind incidence 270° from true north.

Eigenvectors and eigenvalues for the first two pressures modes for a wind incidence of 270° from north are represented in Fig.8. Since the eigenvectors are steady quantities, POD has been directly carried out on the measured pressure coefficients. Due to the different spatial distribution of upper and lower pressure taps, the cubic spline interpolation is required to obtain the differential pressure, which represent the actual load on the structure.

Very important resonant effects have been found. They are dominant in determining the peak responses for most of the wind directions. These effects are strictly related to the damping ratio which has been assumed to be 1% for all considered vibration modes: the monitoring system which has just been arranged on the real structure, seems to show values of ξ even smaller.

The strong influence of resonant effects in determining the global structural response for the case of Braga Stadium is shown on Tab.1, where the mean, quasi-steady and resonant effects are compared,

for 270° from north wind direction, in terms vertical displacement of 6 significant roof points (see Fig.7b)

Node	$\overline{R}$	$g_{qs}^2\sigma_{R,qs}^2$	$\overline{R} \pm \sqrt{g_{qs}^2\sigma_{R,qs}^2}$	$g_{res}^2\sigma_{R,res}^2$	$\overline{R} \pm \sqrt{g_{qs}^2\sigma_{R,qs}^2 + g_{res}^2\sigma_{R,res}^2}$
A	0,1550	0,0250	0,3131	0,3027	0,7275
B	-0,0837	0,0115	-0,1910	0,3076	-0,6486
C	-0,0441	0,0014	-0,0812	0,0433	-0,2555
D	0,0930	0,0052	0,1652	0,0419	0,3101
E	0,0621	0,0092	0,1582	0,2040	0,5238
F	-0,0198	0,0016	-0,0599	0,2018	-0,4709

Tab.1 Comparison of mean, quasi-steady and resonant contributions (node position refers to Fig. 7b)

2.2 Aeroelastic Effects: Aerodynamic Stiffness and Aerodynamic Damping; Pneumatic Effects

Experimental investigation, on scale model of large sub-horizontal coverings [1], gave the possibility of a first comparative analyses of the theoretical values of pressure coefficient with the experimental ones. Since the first studies on the "Stadio delle Alpi" in Turin [2] the aeroelastic model showed that the structural response is lower than that numerically calculated, based on rigid model results (Fig.4). Moreover, the displacement spectra show that the frequency is lower and the "resonant range" is wider than the theoretical ones, as shown in Fig.5. This outlines the role of aerodynamic damping, aerodynamic mass and aerodynamic stiffness. Comparative analyses between wind theoretical spectra and pressure experimental spectra demonstrate that the two models are in contrast, as shown in Fig.10.

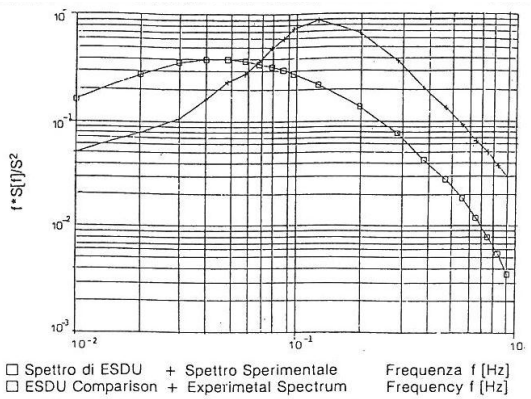

Fig.10 Comparative analyses between wind PSD (ESDU spectrum) and pressure PSD (experimental spectrum)

The experimental pressure spectra presents a peak for frequency of about 0,1 Hz, while theoretical wind spectra for 0,05 Hz (Fig.11). This points out that: (i) the pressure coefficient could not be represented by the mean value and (ii) large flexible roofs are influenced by aerodynamic stiffness and damping; (iii) the structural transfer function has to be "updated" to take into account these phenomena.

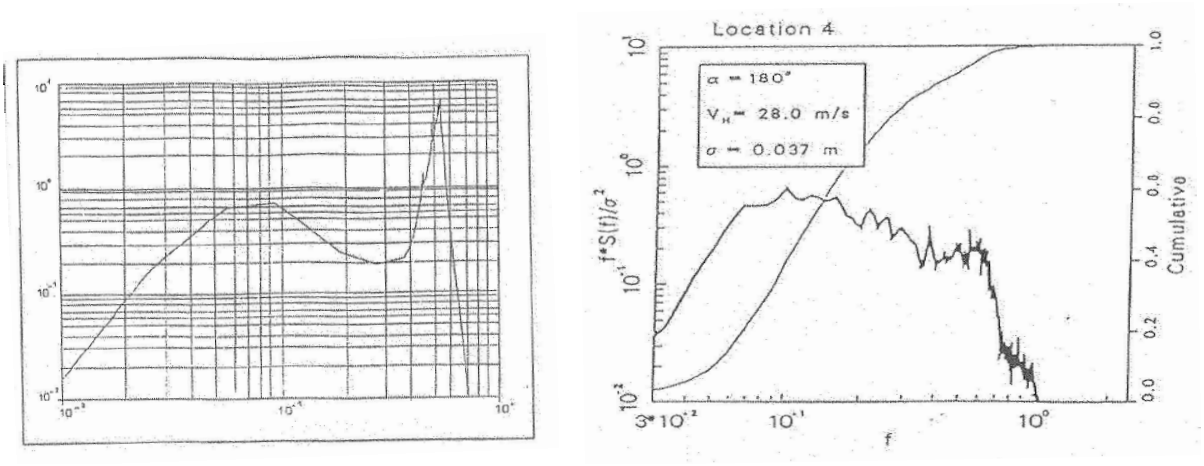

a) *b)*

Fig.11 Displacement DSP of the Turin Stadium large flexible roof: theoretical a) and experimental b)

In addition to the aerodynamic mass-stiffness-damping, many large span roofs are sensitive to pneumatic effects. For such a structure the actual behavior is strongly dependent on the wind interaction phenomenon and on the dimensions of the real openings. In particular the latter aspect represents an important issue in the dynamic analysis of such a roof structure: in fact as a consequence of a small variation in the geometry data, a significant variation in the dynamic response of the whole structure may follow. This is a typical case of great uncertainty in the phase of design and validation of the theoretical as well as numerical analyses that should be carried out for such roof typologies.

The contact between the structure and liquid or gaseous media requires a deformation-depending load model, as shown by Lazzari et al. in [17]; by this way, pressure forces are acting normal to the contact surfaces and friction forces are acting tangential to the surfaces. It was demonstrated that load-deformation relationship can affect direction, magnitude and distribution of the load itself. A load expressed as a scalar function, giving the magnitude of the load, and a unit direction vector, describing the direction of the load, was given. The stress results (Fig.12) show that the structure is strongly influenced by the geometry on which its design is based: it is in the area of the intersection of the two rings that the discontinuities in the stress and strain state occur. The static wind load increases the variation of the forces between elements near each other.

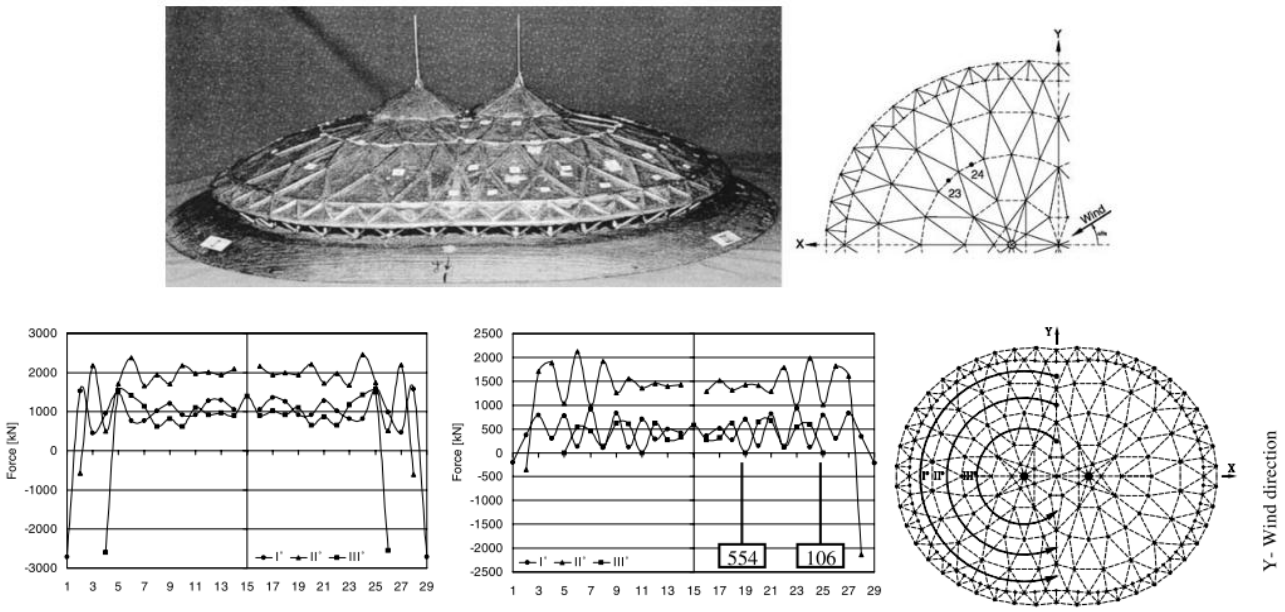

Fig.12 Wind tunnel model of La Plata stadium and stress diagram about the up and down cable under static wind load.

A study on the fluid action on the directly exposed outer surface of roof and on its internal surface as a function of the internal volume changes has been led on the extremely flexible roof of the Montreal Olympic Stadium [18]. Exchange surfaces like access openings represent the connection between the fluid volume enclose on the structure and the external fluid. In case of large openings the fluid field produces point-to-point variable internal pressures acting on the internal side, which are rather small but not negligible when compared with the external pressure level. Such pressures are not generated when the volume is closed.

Nonlinear static and dynamic analyses were performed on Montreal Olympic Stadium [19] and two different loading types were arranged: a conservative surface load for the simulation of loads due to snow and a non-conservative "follower" load for the realistic description of wind action. The final fluid-structure effect (under the hypothesis that internal pressure can be considered as distributed quasi-homogeneously and structural dynamics can be described in a simplified form) is given by an algebraic sum of external and internal pressure due to the structural motion, as shown from nonlinear dynamic analyses tests. In Fig.13 results for infinite exchange surface, 100 m^2 and 50 m^2 exchange surface are presented for permeable structure in terms of stress and displacement at a significant node.

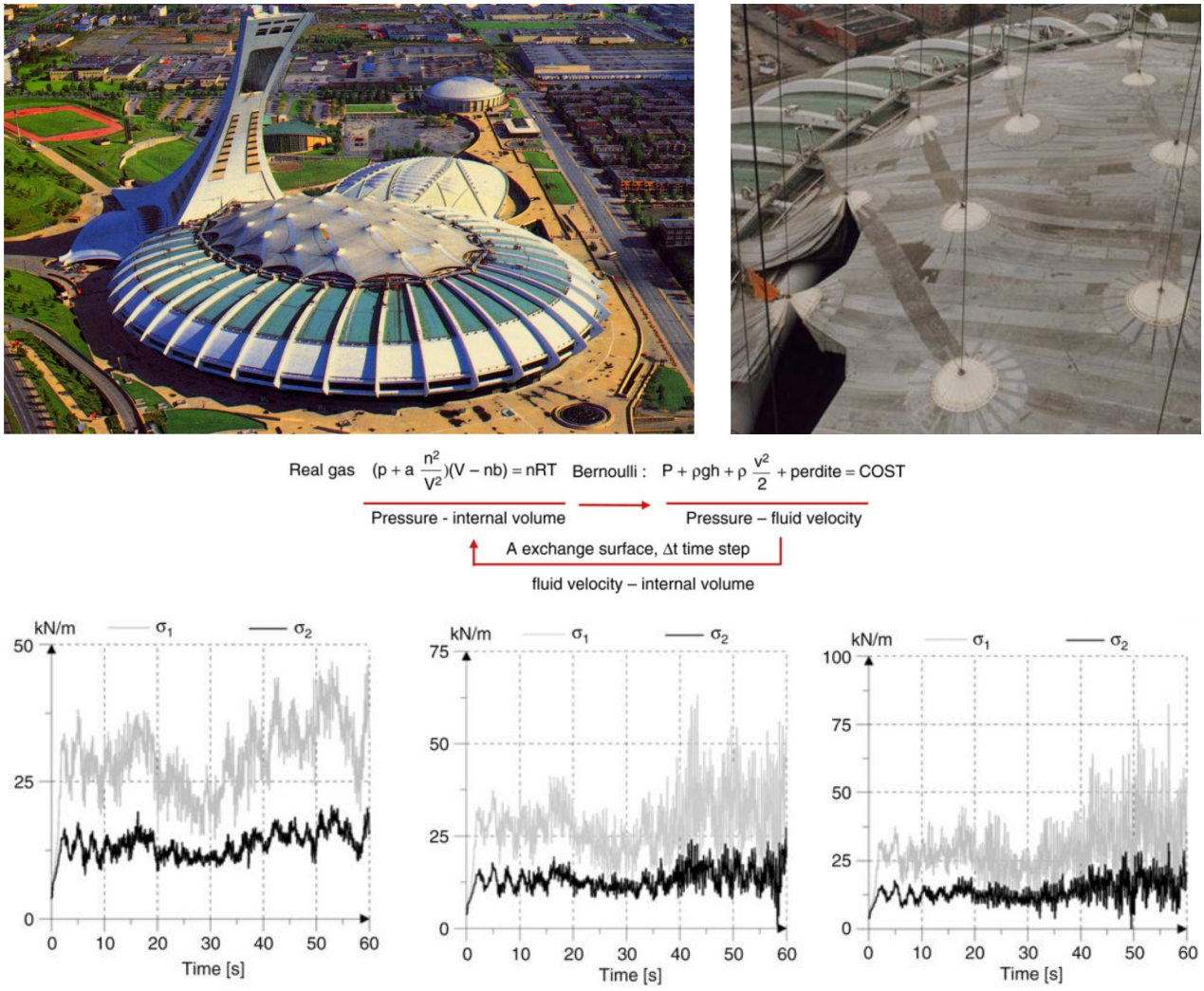

Fig.13 Montreal Olympic Stadium: interaction model between structure and internal volume; stress at node 745 for: a) ∞m^2, b) 100 m^2, c) 50 m^2

In the case of no fluid-structure interaction (Fig.13a), no aerodynamic resonance appears and displacements and stresses remain limited, while the other analyses (Fig.13b-c) shows an onset of aerodynamic resonance that increases as external exchange surface decreases. In the latter hypothesis the structure becomes more stiff and dissipates less energy due to the decreased fluid volume pushed out or the re-called internal volume. Due to the pneumatic effect, large openings presence on structures strongly influence their response.

2.3 Wind-snow interaction

A special analysis of snow loading on the Montreal Stadium (Fig.14) roof was made considering various geometries of the structure during the design of the new roof [18]. Investigations have been carried out from three different models, varying the sag of the roof from 10m, 11.5m and 13m, in order to find a minimization of snow accumulation.

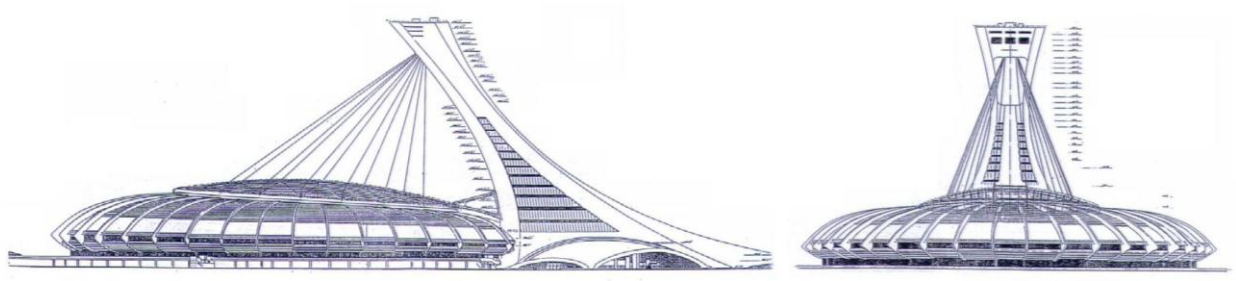

Fig.14 Montreal Olympic Stadium

Finite Area Element (FAE) method was combined with wind tunnel tests on a 1:400 scale model and 30 years ground snow predictions, obtained by data interpolation, were employed to provide an accurate evaluation. A specific study was necessary to investigate the roof behaviour due to the complex geometry and the dependency of the snow loads on many factors, like snowfall intensity, redistribution in speed and direction by the wind, all surroundings affecting wind flow patterns, absorption of rain in the snowpack and depletion of snow due to melting and subsequent runoff.

Models were instrumented with 90° directional surface wind velocity vector sensor covering the surface and additional sensors were installed on the console roof. This analysis permitted to measure local wind speed and direction for 16 wind directions and for an equivalent full-scale height of 1m above the roof surface. Wind speed measurements were converted to ratios of wind speed at the roof surface to the reference wind speed measured at a height equivalent at full scale to 600m.

Structural load cases and local peak loading were not considered as acting over the roof simultaneously. Results of the tests are presented in Fig.15. The case of sag of the roof more than 12m gives separation of the air flow and turbulence in the wake increasing considerably the possibility of snow accumulations. Local over-dimensioning was necessary to avoid the collapse of the structural system as the order of magnitude of the local accumulation in the roof are of 4-15 kN.

Since snow accumulation occurs in the flow-separation regions (critical regions), the geometry modification, due to the accumulation process itself, can strongly influence the aerodynamic behavior of the roof, hence the wind loads and the structural response.

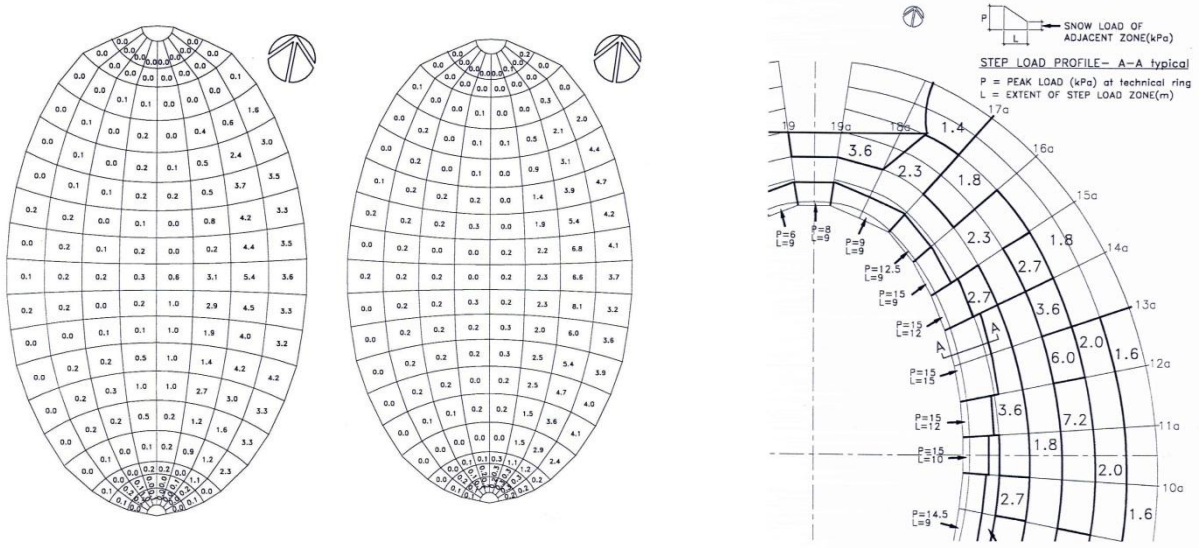

a) *b)*

Fig.15 a) Comparative analyses of snow loading distribution in function of roof shape (10-13m) and b)sliding and wind snow accumulations step loads

Experimental studies on the Montreal Stadium have been carried out for a better understanding of the local failure occurred for a wind load value less than the usual one assumed for the design of these structures combined with snow accumulation [19]. While wind load induces oscillations and deformations and a dynamic formulation is necessary to describe the effects, the load due to the snow accumulation is static and this static effect represents a dominant load for this structures, even reaching as much as 70%-80% of the total load. The experience of Montreal Stadium demonstrated that one of the primary causes of collapse has been attributed to an improper evaluation of the loading conditions and of the structural response.

Significant information has been collected from the observation of such collapse event and numerical analyses on an FE model have been dealt to explain the failure phenomenon due to wind-snow interaction that has occurred in the roof of the Olympic Stadium in apparently unexceptional conditions. In fact the failure happened with a low wind velocity, approximately 19 m/s investing the structure with an angle of 60° from the main axis. The structure was characterized by an antisymmetric dynamic movement and by an oscillation with amplitude of around 5m.

Due to the nonlinear behaviour on the geometry and the complexity of the load simulation, the response of the wide span and flexible roof of the Montreal Stadium was particularly difficult to investigate. Nonlinear analyses results demonstrated large displacements under various conditions, so that significant variations to roof structural stiffness and tensional state close to zero have been found. Moreover low structural stiffness and consequent excess deformability got out from simulations.

Recent works [20] try to numerically model the hazard connected to the snow transport and the deposition by the wind on structures. A detailed computational fluid dynamics (CFD) model was provided and related to wind tunnel data for representative models. Moreover two numerical large eddy simulation (LES) models for transient snow transport by wind were implemented. The approach based on concentration of snow mass for each cell has been followed. Snow movement is adjusted by the combined effect of the local fluid velocity field and gravity; when particles reach the ground solidify, pile up and sometimes topple, so they can change the shape of the boundary of the fluid. At the top of the deposition layer particles are eroded and for a fast fluid flow they are picked up and transported further away. The main components of particles motion under the action of a fluid, like saltation, creping and suspension, can be described by a simple model based on some laws, as for instance the transient update of snow surfaces during simulation after each step, the estimation of erosive or accumulative snow mass flux contribution into or out of the computational cell. The accumulative or erosive snow flux is a function of the snow concentration, the surface normal and shear stress, the particle fall velocity and threshold surface shear stress for particle entrainment. The deposition flux is calculated as a function of the available snow concentration, the snow fall velocity and the velocity flow. The method is based on the balance between erosion and deposition.

3 STANDARD CODES, TESTING AND NUMERICAL TOOLS

This section will focus on analytical and numerical tools to study the previously described phenomena; state of the art and “open problems” are reported.

3.1 Standard codes

Standard Codes usually do not address the problem of the definition of wind induced loads on large roofing system, such as those covering stadia or similar open spaces. Moreover, normally reference is made to very simple and regular shapes, so that no extrapolation can be reliably made to complex geometries or structures following some free form concepts.

When dealing with roofing systems with a very slight inclination with respect to the horizontal plane (e.g. almost horizontal elements), recommendations for free roofs and canopies can be used to give a first idea about the possible loads induced by wind, but no provisions are given for specific cantilevered systems.

One of the few references is represented by Australian Wind Loading Code: the definition of a suitable design load distribution on cantilever roofing systems has been firstly addressed herein in 1989, according to the results reported in a previous paper by Melbourne and Cheung [21]. A peak design triangular load distribution was introduced as a function of the reduced wind speed at the height of the leading edge of the roof (Fig. 16a), e.g. depending on the reduced velocity, V_{red}, defined as:

$$V_{red}=\frac{V_h}{n_1 \cdot d} \tag{6}$$

being d the length of the cantilever roof, n_1 the first mode frequency, V_h the mean wind speed at the height h (top of the roof). The peak pressure coefficients assumed the values:

$$\begin{aligned} C_{p,c}&=5.0 && \text{for } V_{red}\leq 0.4 \\ C_{p,c}&=5.0+2.5\cdot[V_{red}-0.4] && \text{for } V_{red}>0.4 \end{aligned} \tag{7}$$

which values were based on some wind tunnel test results on grandstands fully sealed at the rear, in a typical suburban-urban terrain. The peak design pressure coefficient was related to peak pressure value through the relationship:

$$p_{peak}=C_{p,c}\cdot\frac{1}{2}\rho V_h^2 \tag{8}$$

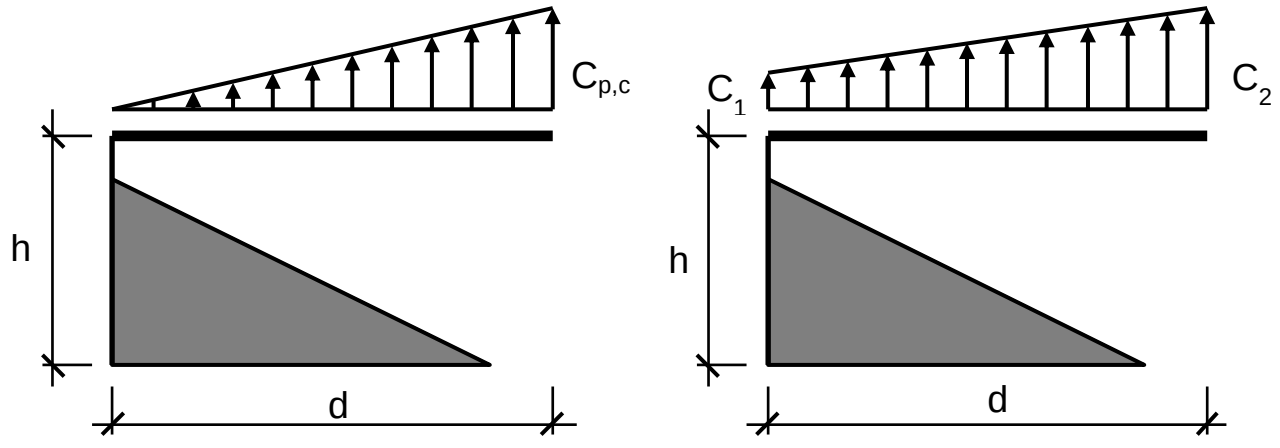

a) *b)*

Fig.16 a) Triangular equivalent static pressure distribution, b) simplified trapezoidal equivalent static pressure distribution

Even if the proposed load distribution took into account only upward loads, some years later Melbourne [22] reported that downward loads as high as approximately half the magnitude of the uplifting ones were possible.

In 2001, Killen and Letchford [23] showed that on central bays the influence of the roof pitch

(within the range ±7°) gave little consequences on maximum moment values; they noted that at low reduced velocities (V_{red} < 0.4) the Australian Wind Loading Code could be unconservative.

Letchford and Killen [24] showed that the assumed triangular distribution could be inadequate for representing the actual peak pressure distributions, especially when no resonant response is expected from the cantilever roof (e.g. at very low reduced velocities). It was observed that the trapezoidal distribution could represent a better way to describe the expected peak panel pressures and to be implemented in wind load codes.

According to literature results, a modification was introduced in the Australian Wind Loading Code (see the latest version: Australian/New Zealand Standard [25]): a trapezoidal equivalent static pressure distribution was introduced (Fig. 16b) and the peak pressure coefficient distributions (obtained through the Load-Response Correlation (LRC) approach by Letchford and Killen [24]) were converted into design pressures by using the design mean dynamic pressure at roof height. A dynamic factor was also introduced to account for possible resonance effects: the dynamic response factor C_{dyn} is higher than unity only for high reduced wind speed (V_{red} > 0.4) and low natural frequencies (n < 1 Hz).

		Height/span h/d ≤ 1.4		**Height/span h/d > 1.4**	
Load direction	Bay position	C_1	C_2	C_1	C_2
Upward loading (–)	Internal	-1.80	-1.10	-1.40	-1.40
	End	-1.30	-1.00	-1.90	-1.10
Downward loading (+)	Internal	0.25	0.15	0.20	-0.15
	End	0.55	0.65	0.20	0.00

Tab.2 Aerodynamic shape factor for isolated cantilever roofs with roof pitch -7° ≤ α ≤ 7° (after Australian/New Zealand Standard 2011)

All the reported values are referred to a fully sealed rear configuration of the roofing system; the gap between roof and grandstand can have a certain influence on mean pressure values, even if it has been shown that it has a little influence on the fluctuating response (Kawai [26]).

A different approach is proposed by the Indian Standard [27], another one of the few codes in which specific recommendations for grandstands are reported. In this case, the design load is evaluated in terms of design pressure coefficients given for the top and the bottom part of the roof, which has been subdivided into four different zones. Values are specified for different incoming wind directions (Fig.17) and they are referred to a three-sides-open configuration, sealed in the rear.

Of course, recommendations reported in wind load codes can be very useful in a preliminary design stage. However, since it has been shown that the presence of upstream structures can significantly affect the wind loading on grandstand roofs, wind tunnel tests represent the crucial tool for an accurate prediction of design loading in such structures.

Wind tunnel tests are also necessary when the designer has either to face geometric configurations largely different from the reference one or to deal with more complex aerodynamic problems. As an example, tests on physical models can be unavoidable in case of a complete covering of a stadium, since the possible influence of the wake produced by the windward roof on the leeward one as well as the effect of the curved geometry of the leading edge of the roof must be taken into account.

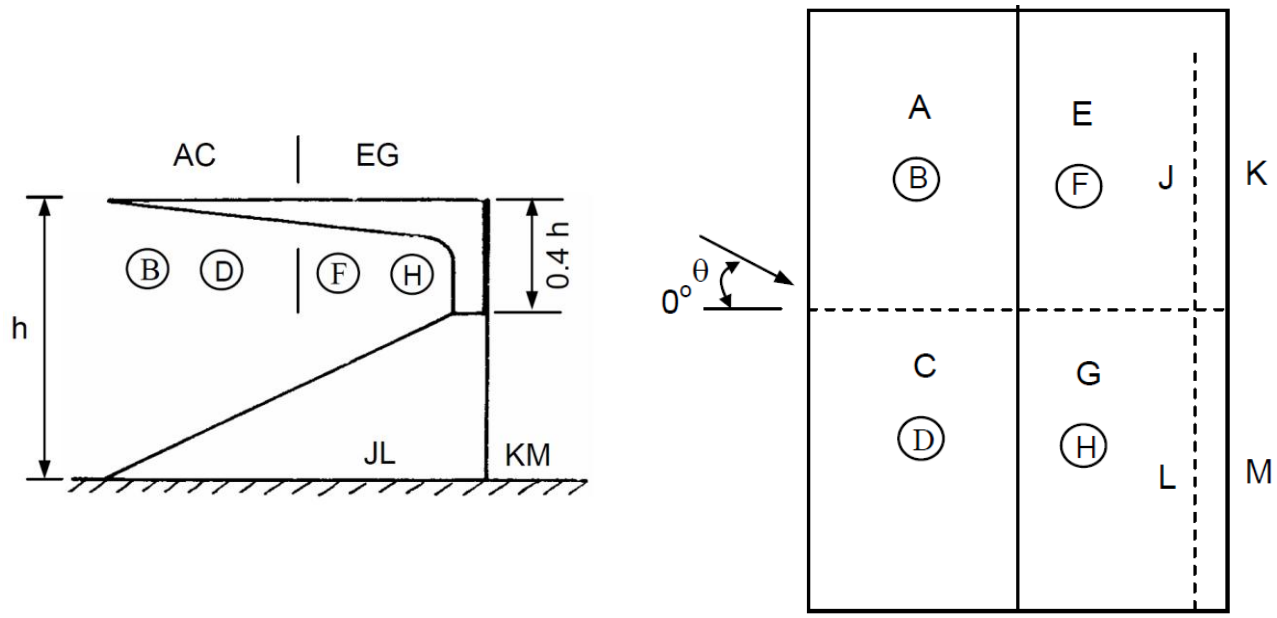

θ	A	B	C	D	E	F	G	H
0°	-1.0	+0.9	-1.0	+0.9	-0.7	+0.9	-0.7	+0.9
45°	-1.0	+0.7	-0.7	+0.4	-0.5	+0.8	-0.5	+0.3
135°	-0.4	-1.1	-0.7	-1.0	-0.9	-1.1	-0.9	-1.0
180°	-0.6	-0.3	-0.6	-0.3	-0.6	-0.3	-0.6	-0.3

Fig.17 Pressure coefficients at the top and bottom of grandstand roofs opened on three sides (roof pitch α up to 5°) [after Indian Standard 875 1998].

3.2 Static equivalent loading combinations

Originally, Davenport [28] defined an Equivalent Static Wind Load (ESWL) as a deterministic load pattern reproducing with a static analysis, one, or perhaps several in the original version, extreme dynamic structural response(s) such as deflections, internal forces or stresses under the fluctuating wind. Its first formulation was expressed as the mean wind load amplified by a unique gust loading factor (GLF) incorporating the background and resonant behaviours of the structure [29-30]. This way of reformulating the complex time/space-dependent distribution of the fluctuating wind load into a deterministic equivalent space-only dependent distribution triggered an endless research on the topic then after. Initially, the concept was developed for the along-wind response of buildings that mainly exhibit vibrations in their first mode [31]. In this case, the GLF is taken equal to the gust response factor (GRF) defined as the ratio of the extreme modal amplitude in the first mode and its mean value [32]. Seminal developments on the formulation of such gust loading factors were reported in [33]-[34]-[35]-[36]. The obvious simplicity of the formulation made it suitable for codification and most standards [37]-[38]-[39]-[40] are based on this approach for the design of vertical structures under several assumptions. Actually, obvious drawbacks are the cases of zero-mean wind loadings and/or responses. Typical examples are across wind sollicitations, due to vortex shedding, and zero-mean modal amplitude for asymmetrical modal shapes as in roof structures. Also, Zhou et al. [41] indicated that the original method gives reliable values for extreme deflections but not for other components, e.g. bending moments and shear forces. In fact, the GRFs may exhibit large sensitivity to the shape of influence functions [42]-[43]. Several studies pushed forward the original idea: Zhou et al. [41] proposed to focus on the base bending moment for the determination of the gust factor, Piccardo and Solari [44] and Kareem and Zhou [45] extend it to more complicated (3D) loading models, Seo and Caracoglia [46] recourse to a database-assisted-design approach. Important inherent limitations of this first approach are: (i) the modal truncation to the first mode, (ii) the need for a simple mode shape and (iii) the range of structural geometry

essentially restricted to vertical structures, partially as a consequence of (i).

Nonetheless, application of the mean wind load amplification concept for rigid and elastic beams supporting flat roof was done by Tamura et al. [42] with wind tunnel tests. Empirical GRFs are provided for displacements, bending moments and shear forces for several buildings models with increasing span ratio and five wind models. Large-span (up to 200 m) elastic beams mainly vibrate in their first mode shape which is more or less similar to the mean displacement validating the applicability of the gust factor approach. For the same type of bearing system of flat roof, Uematsu et al. [47] derived empirical formulas for the ratio of root-mean square and mean modal force coefficient in the first mode as well as the dynamic amplification factor, which are required for the computation of the GRF. These integrate the influence of the height-span ratio, damping-height ratio and turbulence intensity. For long span roofs that behave like elastic flat plate simply supported on four edges under wind loading, Uematsu et al. [48] gave empirical GLFs equal to the GRF of the first modal amplitude. Uematsu et al. [49] apply the same approach for circular flat roof, modeled as an elastic plate, with span up to 150 m under the same assumptions that the structure mainly vibrates in its first mode. For usual rectangular and circular long-span flat roofs, the gust factor method seems to be well-extended.

However, wide span enclosures are usually unique complex structures with complex influence functions (with positive and negative parts) and responding in several low-frequency modes for which other methods have been investigated to produce reliable ESWLs. This makes use of GRF and GLF rather difficult in a systematic way for large roof structure.

A second approach for the formulation of ESWL rose with the studies on the wind loading of low-rise buildings [50]–[51]. In [52] the notion of peak-load pressure distributions is introduced for specific structural responses referred to as “load effects” in his works. To each structural response corresponds specific patterns of pressure distributions that maximize or minimize it in the manner of an influence line or influence surface, in a static analysis. As an important conclusion, the set of ESWLs considered for the design has to reproduce, in a conservative way, all extreme structural responses. The minimum and maximum values that may reach any response define the envelope. An important breakthrough was achieved with works of Kasperski [53] who derived the mathematical formulation that defines an ESWL as the most probable wind load pattern associated with an extreme value of a specific response. The assumption is a Gaussian wind field and the proposed method termed the load-response correlation (LRC) method [54] is limited to structures with a background and weakly nonlinear behavior. More precisely, the LRC method gives the load pattern producing an extreme value (min or max) of the (zero-mean) fluctuating response. This works also emphasizes that the design wind load necessarily has to be expressed by adding and subtracting ESWL to the mean wind loading. This is all the more relevant as the structure has a complex structural and aerodynamic behavior as wide-span enclosures. Again, this is typically important, for the responses that correspond to influence functions with positive and negative parts that may reach extreme values associated with minima of the wind loads. The LRC method has the main advantage to provide meaningful realistic load for any considered response.

For the quasi-static analysis of a circular flat roof, Uematsu [55] compared the results of the LRC method applied to the wind pressure field model, that was fitted on the data with (i) a properly selected snapshot of the wind pressure field and (ii) results of the LRC method applied to the measured pressure field. The last two wind loading patterns are close while the former shows acceptable overestimation as a consequence of the simplified wind loading model. For cantilevered grandstand roof, improvements of the design load patterns provided in the Australian code were benchmarked with those obtained with the LRC method [24]. Actually, the LRC method has been incorporated in the ISO-document [39] for the design of low-rise buildings [56].

Even if not formulated as such, Davenport [57] sketched the use of inertial forces as external

ESWLs for the dynamic analysis of long-span bridges. An inertial force statically applied to the structure produces a deflection affine to the corresponding mode shape. It is well-suited to structures with a dominating resonant behaviour. In case of an intermediate background-resonant structural behavior, Holmes [58] formulated the ESWL as an addition to the mean pressure field of an SRSS combination of the (background) load pattern obtained with the LRC method and a resonant load pattern resulting from the first modal inertial force. This formulation was initially derived for structures that exhibit a resonant behavior only in their first mode and is termed "effective static load distribution" in his work. Design of the Stadium Australia and the Sydney SuperDome was based on this method [59]. For the background component of the ESWL, comparisons are made between a direct approach in which instantaneous pressures producing extreme responses are picked up and those obtained with the LRC method. The authors advised to use the second approach because it produces, from a statistical point of view, more reliable load patterns than those obtained with a single snapshot. The formulation was pushed forward by Zhou et al. [60] for horizontal structures that may exhibit resonant responses in several modes but neglecting modal response correlations. Other ways to combine the different contributions (mean, background and resonant) of an ESWL is a weighted addition of each part. This is discussed in [61] with extension to modal response correlations and by Holmes [62] which introduces, in the weighting coefficients, the corresponding peak factor of each contribution (background and resonant). These developments are classified as load combination (LC) techniques [63]. The LC technique has been applied to a wide range of roof structures as cylindrical shell models [64] or long-span roof structures, for example to the 486 m long roof of the Shenzhen Citizens Centerwith in China [65].

Recently, Blaise and Denoël [66] have introduced the displacement-response correlation (DRC) method in the context of a full dynamic analysis in the nodal basis. This method is an extension of the original LRC method limited to nodal static analysis. No combination of background and resonant parts are necessary because the ESWL derived with the DRC method includes naturally both contributions.

Beyond the concept of ESWL, is that of "envelope reconstruction problem" (ERP) aiming at determining a set of optimal static loadings that globally reproduces the whole envelope that would be obtained with a formal buffeting analysis. Indeed, all these ESWL methods have the same limitation that an ESWL is associated with only one structural response. This has been pointed out by Repetto and Solari [63] in the case of the GF technique as well as the LC technique. For design purposes, a set of ESWLs has to be determined in order to accurately reproduce the entire envelope. The original approach was to consider the ESWLs associated with some specific responses of major importance, e.g. first modal amplitude for high-rise buildings. As explained in [53] and mathematically formalized in [66], the reconstructed envelope of responses under a set of ESWLs will match perfectly the real one if all ESWLs are considered or a subset may be used if some responses are perfectly correlated. This indicated that if a minimum number of ESWLs is envied for the analysis, they have to be adequately chosen to provide an approximation of the entire envelope as close as possible for a chosen level of accuracy. A global loading technique has been derived in [63] for vertical structures that makes the ESWL independent of the response considered. The idea is to impose that several (and not only one) responses have to reach simultaneously their extreme values.

Other methods use combinations of eigenmodes of the fluctuating wind pressures [67] to establish representative ESWLs independent of the structural responses. The universal ESWL introduced by Katsumura [68] is a combination of eigenmodes calculated by covariance proper transformation [69]-[70]-[71]. These methods fall within the scope of POD decompositions and are discussed in the following section. An important feature of this unique loading is its ability to simultaneously reproduce extreme responses. Even if the concept is appealing, the method seems to be not

straightforward. Indeed, former studies [72]-[73]-[56]-[74] revealed several drawbacks of the universal ESWL as erratic load patterns, deficient response estimations and suggest some ways to improve its reliability. Recent application of the universal ESWL [75] however confirm its effectiveness and applicability to a wide class of structures. Chen and Zhou [72] used ESWLs computed as the CPT loading modes amplified by the square root of their principal components. They applied them independently and responses under each ESWLs are then combined with an SRSS scheme.

Zhou et al. [74] combine ESWLs obtained with the LRC method to produce one that simultaneously targets several responses. Again, weighting combinations are obtained by trial and error which makes its automatic application difficult. Seeking also the envelope reconstruction problem, Fiore and Monaco [76] propose a global wind loading obtained with combinations of spectral eigenfunctions. Drawback remains the necessary preselection of a user-defined number of structural responses to tune the combination coefficients.

Recently, seeking to derive a more general basis of static loadings to be combined for the ERP, Blaise and Denoël [66] have proposed the concept of principal static wind load (PSWL) obtained as a result of the singular value decomposition of all of the ESWLs associated with all responses. They compared CPT loading modes with PSWLs for the ERP and demonstrated that the second basis of loadings performs better as a result of the formal way it is derived. For the large stadium roof of Marseille, Blaise et al. [77] combine these PSWLs using Monte-Carlo simulations and based on the maximization of a chosen indicator of convergence to the real envelope. As appealing as it could be, no automatic procedure for establishment of the weighting coefficients is given but through the indicator of convergence, the proposed technique is adaptive in order to meet specific envelope reconstruction requirements. An illustration of the method is given in the next paragraph.

In conclusion, the concept of equivalent static wind analysis with deterministic load patterns aiming at reproducing as close as possible the responses that would be obtained with a formal buffeting approach has been enhanced through the decades in order to improve its reliability. For large roof structures typically wind-sensitive and responding in several, possibly coupled, low-frequency modes, the GLF and GRF concepts seem to be not adapted. Depending on the type of structural analysis performed (quasi-static or resonant), combinations between the mean, background and resonant load patterns seem to be preferred. Combinations may be realized as an SRSS combination or a weighted addition of each part with several peculiarities. Most recent works focus on the definition of a more general basis of static load patterns (not dependent on specific responses) and among several propositions, combinations of them appear to remain quite challenging in order to match as close as possible the real envelope with automatic procedures.

3.3 Illustrations of PSWLs

The envelope reconstruction problem is illustrated with the Marseille velodrome in France, see Fig.18a. The dimensions are 258×256×74meters. The structure is a rigid lattice composed of hollow tubes and the roof is covered with a high density polythene membrane. The aerodynamic loading characterization has been realized by wind tunnel simulations at the "*Centre Scientifique et Technique du Bâtiment*" at Nantes, France, see Fig.18b.

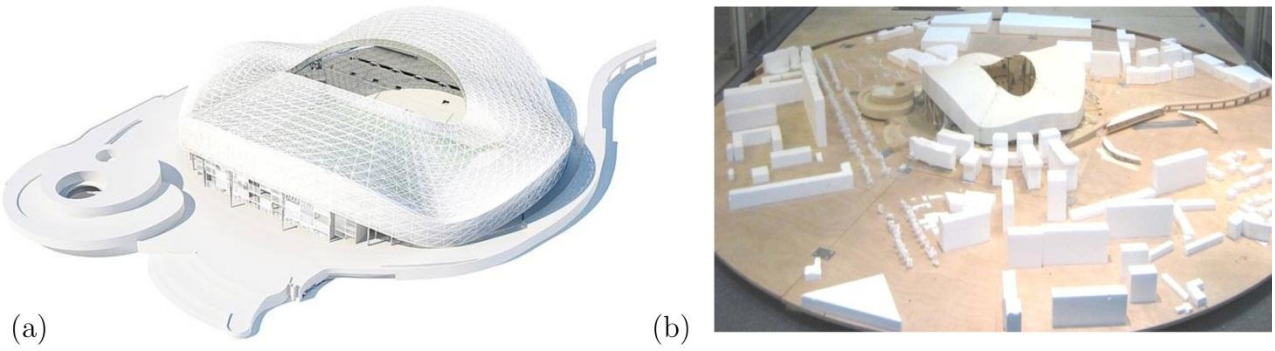

Fig.18 (a) Computed graphic of Marseille's velodrome, France and (b) 1/250-scaled model (rigid) of the stadium (courtesy of CSTB).

Illustrations are provided exclusively for the most restrictive wind direction, 220° [77]. Figure 19 depicts the first four CPT loading modes $\boldsymbol{p}_k^c$ and PSWLs $\boldsymbol{p}_k^p$.

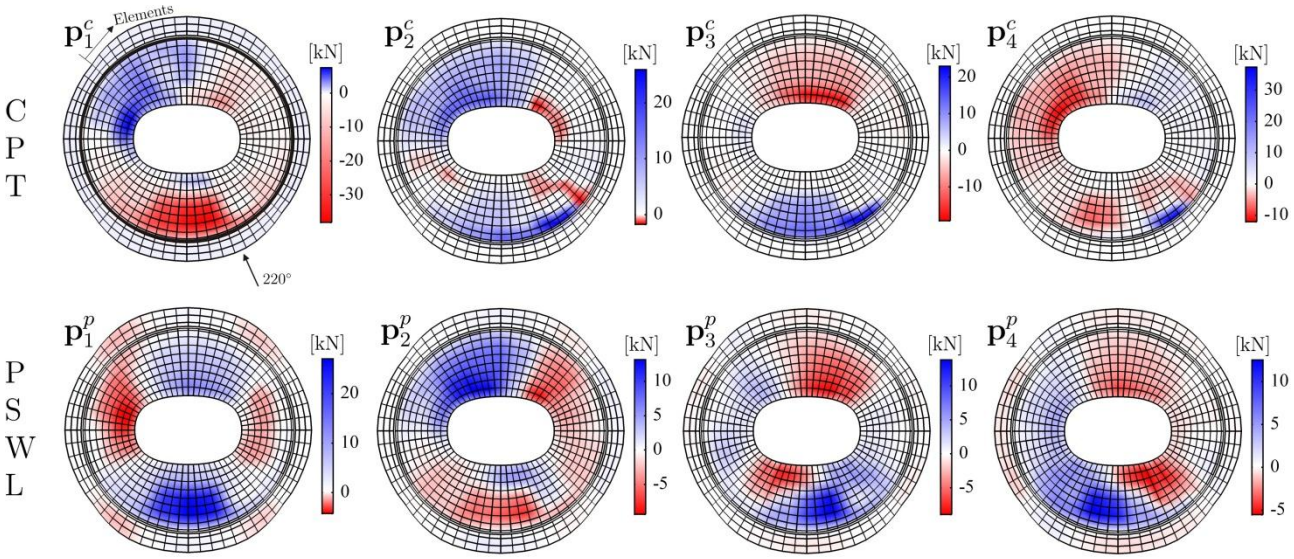

Fig.19 Global vertical external nodal forces of the first four CPT loading modes (upper part of the graph) and principal static wind loads (lower part of the graph). 120 circumferential beam elements are identified in bold on the graph of $\boldsymbol{p}_1^c$.

Both have been normalized such that the corresponding static response $\boldsymbol{r}_k^c$ (resp. $\boldsymbol{r}_k^p$) is somewhere tangent to the zero mean symmetric envelope ($\boldsymbol{r}^{min}$; $\boldsymbol{r}^{max}$) obtained with a formal buffeting analysis with the assumption of gaussianity. Both types of loading modes cover large parts of the roof with similar magnitudes. The main difference is that CPT loading modes do not incorporate the behaviour of the structure while PSWLs does. The first CPT loading mode and the second PSWL present a similar pattern but with a shift in the magnitude.

Establishment of the PSWLs basis results in the SVD operation on 68832 ESWLs previously computed using the method in [61]. Indeed there is 5736 beam elements with six internal forces (axial force, two bending moments, two shear forces and torque). The envelope reconstruction of axial forces N is illustrated with 120 circumferential beam elements localized at the outer perimeter of the roof and identified in bold in Fig.19. Figure 20a shows the static responses $\boldsymbol{r}_k$ under each

loading modes (CPTs or PSWLs) of Fig.19 within the envelope ($\boldsymbol{r}^{min}$; $\boldsymbol{r}^{max}$). Figure 20b illustrates the sequential reconstruction of the envelope defined by ($\tilde{\boldsymbol{r}}_k^{min}$; $\tilde{\boldsymbol{r}}_k^{max}$) = (min ($\tilde{\boldsymbol{r}}_{k-1}^{min}$; $\boldsymbol{r}_k$; -$\boldsymbol{r}_k$; 0); max ($\tilde{\boldsymbol{r}}_{k-1}^{min}$; $\boldsymbol{r}_k$; -$\boldsymbol{r}_k$; 0)). With this formulation, with the k^{th} reconstructed envelope is associated 2k loading cases. Upper (resp. lower) part of each graph of Fig.20b depicts the reconstruction of the max (resp. min) part of the envelope $\tilde{\boldsymbol{r}}_k^{c,max}$ (resp. $\tilde{\boldsymbol{r}}_k^{p,min}$) that would be obtained with static analyses under the sequential applications of the CPT loading modes (resp. PSWLs). Better estimation of the envelope is reached with the PSWLs than with the CPT loading modes. However, after the first two, considering more and more PSWLs or CPT loading modes does not improve significantly the reconstructed envelope because no combination is considered and the loading modes are ordered by importance due to the SVD operation. Nonetheless, SVD operation produces orthogonal vectors that are well-suited for combinations. Thus, a way to ameliorate the envelope reconstruction is to consider also combinations of the loading modes rather than their sequential application. Any combination of the CPT loadings modes or PSWLs produces a new static loading denoted by $\boldsymbol{p}^{s_c}$ (resp. $\boldsymbol{p}^{s_p}$) associated with structural responses $\boldsymbol{r}^{s_c}$ (resp. $\boldsymbol{r}^{s_p}$). The successive static analyses under each combination of the CPT loadings modes and PSWLs produce a sequential reconstruction of the max (resp. min) part of the envelope $\tilde{\boldsymbol{r}}_k^{s_c,max}$ (resp. $\tilde{\boldsymbol{r}}_k^{s_p,min}$). The combination coefficients are obtained with Monte-Carlo simulations. Random combinations of the first two, three or even four CPT loading modes do not bring a significant better estimation of the envelope than just their sequential application. Random combinations of the PSWLs allow to improve significantly the reconstructed envelope even if four restricted parts of the envelope are still largely underestimated which indicates that more PSWLs may be considered. This demonstrated that the CPT loading modes failed to be an optimum basis for the envelope reconstruction envelope because they do not integrate the structural behaviour of the structure.

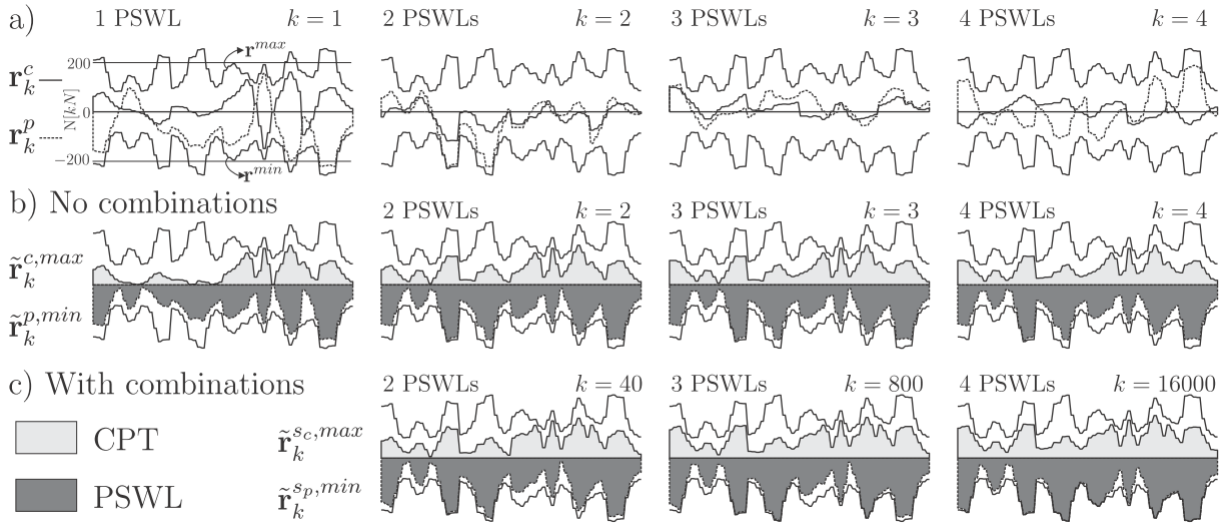

Fig.20 Static responses under the first four (from left to right) CPT loading modes (upper part of each graph, lines) and the PSWLs (lower part of each graph, dashed lines) within the zero-mean envelope (a). Envelope reconstruction, max and min, without combinations of the CPT loading modes and PSWLs, respectively (b). Envelope reconstruction, max and min, with combination coefficients of Monte-Carlo simulation of the CPT loading modes and PSWLs, respectively (c)

For design purposes, a finite number of representative design load cases has to be identified, especially that within all possible combination coefficients, only a fraction allow to further increase the accuracy of the reconstructed envelope. Number of PSWLs that have to be kept and selection of

combination coefficients is addressed in [77].

3.4 POD and other approximation tools

The Proper Orthogonal Decomposition (POD) technique expresses a set of correlated random processes as a combination of orthogonal functions modulated by uncorrelated stochastic processes [78]-[79] This method, termed also the Karhunen-Loeve expansion [80] and belonging to Principal Component Analysis (PCA) [67], has been widely applied in wind engineering as an understanding, simplification, modeling and simulation tool for the structural analysis [81]-[71]-[82]. Data processing techniques may be sorted into two families depending on the correlated random field on which POD is applied, e.g. the oncoming wind velocities or the aerodynamic pressures acting on the structure.

In both cases, deterministic orthogonal shapes are extracted from the complex timespace representation of a wind turbulence (resp. loading) field that may be obtained with wind tunnel measurements, computational fluid dynamics or full-scale measurements. These modes are sometimes termed wind blowing mode [83] or (wind) loading modes, respectively. Each wind mode is amplified by its principal component uncorrelated with the others. Linear combinations of a limited number of wind modes with their principal components are supposed to reproduce accurately, in a mean square sense, the entire wind field in time and space.

Although partly driven by the drastic need to compress wind-tunnel data in 1960's-1980's due to computer storage limitations, POD has been constantly used in order to provide a sound understanding of the wind and pressure fields.

First applications cristallized with the Covariance Proper Transformation (CPT) consisting in the diagonalization of the zero-lag covariance matrix of the wind field. The CPT produces wind modes that are only space-dependent with principal components uncorrelated only for a zero-time lag. The spectral Proper Transformation (SPT) consisting in the diagonalization of the power spectral matrix of the wind field produces space-frequency dependent wind modes and principal components that are uncorrelated for any time lag. Therefore, the SPT provides a higher reconstruction rate of the original wind field than the CPT does. Nevertheless, under some circumstances, CPT and SPT may produce similar wind modes [84] with a much heavier computational cost for SPT, though.

A short description of POD applied to the turbulence field is first discussed. Usually, the turbulence field is modeled by a zero mean weakly stationary Gaussian 3-V (variate) (longitudinal, lateral and vertical turbulence components) and 4-D (dimensional) (three spatial coordinates plus time) random process. In the frequency domain, the cross-power spectral density functions describe the space-time characteristics. Several authors have proposed models using POD for simulation of 1-V 4-D [83-85], 1-V 2-D [86] and 3-V 4-D [87;88] wind velocity fields.

These simulation methods based on POD are typically well suited to line-like structures such as buildings or bridges. Indeed, using well-known closed-form expressions of aeroydnamic admittances [89], aerodynamic pressures may be computed with the simulated turbulence wind field. However and even if not clearly stated, an aerodynamic admittance is given in [55] for a circular flat roof. Also, Han and Li [90] used the CPT to reconstruct and interpolate wind velocities on a tensile cable-membrane large roof structure, the Foshan Century Lotus Stadium (outside diameter of 300 m). Actually for wide-span enclosures, the wide variety of shapes, the 3-D geometry of the structure, and the particular aerodynamic signature of such large structures, conspire to make the determination of a general expression for the aerodynamic admittance quite challenging, if not vain. Consequently, a proper recourse to the aerodynamic pressure field is preferred.

Application of the POD directly to the aerodynamic pressure field on a bluff body was first investigated by Armitt [91]. Using the CPT truncation of wind-tunnel measurements, [68] reduced the computational effort implementing their covariance integration method for static analysis of low-rise buildings. For the same type of structures, effects of integration of only a part of or all panel pressures for the CPT [92], possible simplifications of the CPT modes based on the influence functions [93] and presence of internal pressures due to openings in the buildings [94] were investigated. This latter study compared the experimental CPT blowing modes with those resulting from the modeling of the covariance matrix with a decreasing exponential and identical variances on the diagonal [95]-[96]. In [97] was clarified that the application of the CPT must be made on the fluctuating aerodynamic pressure without the mean values which otherwise would introduce distortion in the loading modes.

The importance of the POD tool in determining wind loads in a generalized and simplified way was highlighted in [98]-[99]. Wind-induced dynamic behavior on single-layer latticed dome was investigated by Uematsu et al. [47] using CPT loading modes. Nine configurations of dome geometry with three different increasing rise-span ratios were considered to model low-, middle- and high-rise domes, respectively. Physical interpretations of the CPT loading modes are done using the quasi-steady theory [100] and analytical equations for the loading modes are proposed with expressions that could be generalized to other dome shapes. The wind pressures acting on the structure for the analysis were generated using proposed formulations of symmetric and anti-symmetric loading modes. Combination coefficients are necessary to derive the loading modes and they have been tuned for the specific experiment. The LRC method allows to compute ESWL and for the background contribution of several large roofs, Holmes and Wood [59] simplify the computation of the correlation coefficient between load and response using the CPT. Indeed, CPT loading modes have been used to establish ESWLs [68]-[72]-[101] compute CPT wind modes on hyperbolic paraboloid shaped roofs from wind tunnel measurements. For the Shenzhen Citizen Center, Liu et al. [102] compare aerodynamic pressures measured in full scale and those reconstructed with CPT modes derived from recorded pressures in wind-tunnel.

Benfratello and Muscolino [103] used the SPT method to perform the stochastic analysis of an MDOF structure in order to evaluate the statistical moments with possible inclusion of the quadratic terms in the aerodynamic forces. Solari and Carassale [104] introduced the Double Modal Transformation (DMT) method to analyze the structure in the modal basis using loading modes obtained with CPT or SPT methods. The DMT method allows to compute the dynamic response of each structural mode under each loading mode and finally, the structural response is obtained, in an elegant way, with a double linear combination of some pairs of structural and loading modes [105]. Although apparently optimal, from a computational point of view, it appears to be efficient only if the mode shapes and loading modes are known in closed form. Essentially, this concerns line-like structures for which aerodynamic pressures may be directly obtained with a turbulence field characterized by a simple analytical model. The DMT method has been applied to tall buildings [106], and long-span bridges [107]. Concerning widespan enclosure, Blaise et al. [108] discussed different structural analysis methods, including the DMT, from wind-tunnel pressures on the stadium roof of Lille (France). It is reported that the cross-modal participation matrix mixed between structural and CPT loading modes is fully populated. Interesting orthogonality properties between the structural and wind modes are thus hardly exploitable. Moreover, they suggest to fit probabilistic models on the principal components of the SPT. This idea is appealing since no coherence function has to be considered in that case; however the fitting of the space-frequency dependent loading modes appears to be difficult to fit with a general analytical model.

As a matter of fact, concerning applications of the POD as a tool for the analysis of wide-span enclosures, few studies are reported. As mentioned by Chen et al. [109], the environment and the shape of the wide-span roof play a determining role in the characterisation of the wind loads and

every new wide-span roof requires specific studies.

3.5 Direct integration of experimental time histories (Montecarlo simulations)

Wind tunnel tests provide deterministic time histories of the aerodynamic pressure with several taps on the structure's roof. In early ages of wind tunnel engineering, direct integration of these measured pressures for a structural analysis with classical integration methods [110] was not straightforward because of the limited number of taps that could be used synchronously, the sampling rate or the duration of measurements. Indeed, a sparse tap layout or no information about the coherence between them would provide inaccurate results or even large overestimations in case of analysis performed with a wind measured field assumed to be perfectly coherent [6]. Because the full-scale sampling rate is even smaller than the wind-tunnel sampling rate, inaccuracies in the dynamic modal analysis such as period elongation and excessive numerical damping [110]-[111] may only be avoided with a very high wind-tunnel sampling rate or a small scale model.

Based on simplified models for PSD and (usually serious) hypothesis on correlation, the set of measured pressures was used to simulate the wind action on the entire structure which was then used in a time-domain analysis. This is described in [112] for Rome's Olympic Stadium which is a large tensile structure that behaves nonlinearly, another reason why time-domain analysis is required [113]. Vickery and Majowiecki [2] have studied the design of the experiment in order to provide a satisfactory space description of the wind loading that may be used directly for time-domain analysis. They highlighted also non Gaussian features of quasi-static responses and recommend a time-domain approach to correctly compute their extreme values. Direct integration of time histories for static and dynamic analysis is also reported in [114] for a hanging roof with geometrical nonlinearity.

From a statistical point of view, each window of measurement is a sample of a Monte-Carlo simulation which may be used for a one-shot deterministic time-domain structural analysis. With this option, probabilistic aspects are limited to some statistical treatment, after the structural analysis is performed, should several time windows be considered. Statistical processings are mainly done for the characterization of extreme values for the structural design.

Augusti et al. [115] describe several options for its calculation or approximation. Biagini et al. [116] compute extreme values of structural responses using the Gumbel method. It consists in the division of the full-time history in 10-min time windows and the selection of the extreme values on each of them. The distribution of the extreme values is then characterized and design values are defined [117]. Another simplified approach consists simply in averaging the extreme values on each 10-min time window [107]. In general, these methods are typically time-consuming because they require a large amount of simulations in order to provide reliable estimates of extreme values. On the other hand they allow to easily compute different peak factors for maximum and minimum structural responses accounting for the non Gaussian pattern [49]-[118] of the pressure field, a feature typically important for large roof structures.

Instead of direct integration of wind pressure histories in the time domain, an alternative analysis method consists in transforming the pressure histories into the Fourier domain and in performing the structural analysis in this domain [119]. One advantage of this approach is to get rid of the transient component of the response, offering thus direct access to structural responses of interest. For a large roof structure that behaves linearly and within a Gaussian framework, Blaise and Denoël [118] compared deterministic timeand frequency- domain analyses. They recommend the second approach for the flexibility in pre-processing the time-histories in order to ensure a reliable analysis.

Besides, these analysis methods based on a complete time or frequency domain representation of the pressure field, there is a wide variety of methods where probabilistic models could be fit on the measured pressure or on any of its by-products. For instance, Blaise and Denoël [111] discussed

and compared various ways to fit a probabilistic model on the measured data. For several reasons, it turns out that an interesting and accurate way to perform the structural analysis is to project the pressure field into the modal basis and to fit the generalized forces with a suitable probabilistic model. After comparison, this method seems to be superior to a probabilistic fitting of the full pressure field or the CPT and SPT representations.

In the future, we could expect that direct integration of pressure field histories will be yet more commonly applied thanks to increases in wind-tunnel frequency rate, available synchronous pressure taps and computational power. However, it is recommended that the raw data be inspected with care as a blind application of these integration methods could suffer from some measurement imperfections. Definitely, any pre- or post-processing or probabilistic fitting aiming at smoothing the limited information collected in the wind-tunnel presents also appealing attributes.

3.6 Stochastic sensibility analyses of wide span enclosures to wind action

3.6.1 Introduction

In wind-resistant structural design practice, the consideration of the dynamic wind loads on long-span roofs conducts to a complicated failure equation since the wind load distribution on the structure is a time and space random process.

As introduced in previous sections, in 1992, Kasperski [53] proposed the load-response-correlation (LRC) method where the most probable load distribution to generate a specific maximum response is obtained. Kasperski defined the design wind load distribution as the load pattern which causes a specified maximum response r_{imax} of quasi-static linear system (Fu et al. [120] have shown later that the method can be extended to the total dynamic response, i.e. background and resonant components).

$$r_{imax}=\mu_{r_i}+q\sigma_{r_i} \tag{9}$$

In Eq. (9) q is the peak factor or the number of standard deviations by which the peak exceeds the mean value (a value around q=3.5 is usually selected for Gaussian processes) and σ_{r_i} is the standard deviation of r_i. In the LRC method the design load pattern for the specific maximum response is computed as [53]:

$$P_k^*=\mu_{p_k}+q\rho_{r_ip_k}\sigma_{p_k} \tag{10}$$

where μ_{p_k}, σ_{p_k} are the mean value and the standard deviation of the wind load P_k and $\rho_{r_ip_k}$ is the correlation between the response r_i and the load P_k. It can be shown that Eq.(10) can be also written as

$$\mathbf{P}^*=\boldsymbol{\mu}_\mathbf{P}+q\frac{\mathbf{C_P f_i}}{\sqrt{\mathbf{f_i}^T\mathbf{C_P f_i}}} \tag{11}$$

where $\mathbf{C_P}=E[(\mathbf{P}-\boldsymbol{\mu}_\mathbf{P})(\mathbf{P}-\boldsymbol{\mu}_\mathbf{P})^T]$ is the covariance matrix of the wind loads $\mathbf{P}$ and $\mathbf{f_i}$ is the influence vector of the response r_i so that

$$r_i=\mathbf{f_i}^T\mathbf{P} \tag{12}$$

To be used as a load distribution in the context of reliability based analysis, the load pattern of the LRC method has to be introduced in the failure equation so that the other random variables and the target safety index β^* can be considered. In this way it is obtained: a) a general and objective criterion for selecting the specific response r_i on which the wind load distribution is based; and b) the consideration of the different failure modes, capacity of the members and target reliability in the definition of the design load pattern.

The purpose of this section is to show some tools to determine the most probable wind pressure values and distribution at failure viewing them as a random process (in general, from experimental data obtained in scale models) for wide span enclosures. This question is addressed here using one-dimensional example. Let us assume that the beam in **Errore. L'origine riferimento non è stata trovata.**must be designed for wind loads $\mathbf{P}(t)=\mathbf{P_0}+\mathbf{P}'(t)$.

The terms $\mathbf{P_0}=\mathbf{p_0}wA$ are the mean value of the wind loads during a windstorm of specific duration τ (for example τ=1hr), $w=1/2\rho\upsilon_\tau^2$ is the wind mean pressure, υ_τ is the mean wind speed during the period τ in the region outside the influence of the beam, A is the influence area corresponding to each force P_0, p_0 are the mean wind pressures coefficients along the beam during the period τ. Since for structural design it is required the maximum wind load for the life cycle of the facility T_R (for example T_R=50yr), w is also a random variable (i.e., the maximum value in T_R years). Usually a maximum Type I probability distribution and a coefficient of variation around $\delta_w = 0.30$ is considered for the maximum wind loads during lifetime [121].

The terms $\mathbf{P}'(t)$ represent the variation of the wind loads around its mean value $\mathbf{P_0}$ during the windstorm. It is assumed that $\mathbf{P}'(t)$ is a stationary random process but not necessarily Gaussian with covariance matrix $\mathbf{C_{P'}}=\mathbf{C_{P'}}(1/2\rho\upsilon_\tau^2 A)^2=\mathbf{C_{P'}}w^2A^2$. In general, $\mathbf{C_{P'}}$ is computed from experimental data obtained with scale models in wind tunnel.

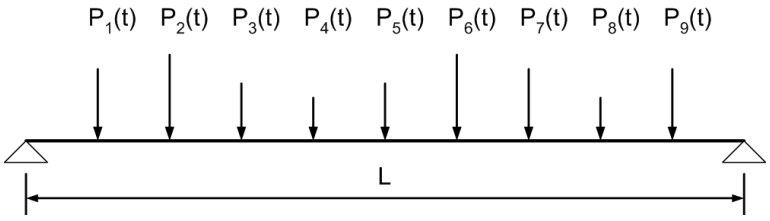

Fig. 21. Example of a beam under wind loads

The maximum response r_{wi} (bending moment, shear, stress, etc) at a section i of the beam of **Errore. L'origine riferimento non è stata trovata.** due to the wind loads can be computed as:

$$r_{wi}=\mathbf{f_i^T P_0} + q_i\sigma_{ri} \tag{13}$$

where $\mathbf{f_i}$ is the influence vector of the response r_i, σ_{ri} is the standard deviation of the response r_i due to the random wind load with zero mean $\boldsymbol{P'}(t)$ and q_i is the peak factor for the stationary wind load response that is not necessarily Gaussian. This consideration is important since wind load processes are usually non-Gaussian. For example, wind pressure fluctuations around low-rise buildings are mainly non-Gaussian [122]. The standard deviation of the response r_i can be computed as

$$\sigma_{ri}^2=E[r_i r_i^T]=E[\mathbf{f_i^T P' P'^T f_i}]=\mathbf{f_i^T}E[\mathbf{P' P'^T}]\mathbf{f_i}=\mathbf{f_i^T C_{P'} f_i}=\mathbf{f_i^T C_p f_i}w^2A^2 \tag{14}$$

The mean and standard deviation of the peak factor q, μ_q and σ_q, for non-Gaussian process can be

analytically computed as proposed by Kwon and Kareem [122] and by Floris and Iseppi [123]. The mean and standard deviation of the peak factor q, μ_q and σ_q, for Gaussian process has been obtained using asymptotic expressions by Davenport [124]. Using Eq. (14) the maximum response r_{wi} (Eq.13) due to the wind loads can be computed as

$$r_{wi}=\mathbf{f}_i^T\mathbf{P}_0+q_i\sigma_{ri}=\mathbf{f}_i^T\mathbf{p}_0 wA+q_i\sqrt{\mathbf{f}_i^T\mathbf{C}_{p'}\mathbf{f}_i}wA \quad (15)$$

In the proposed reliability-based method, the equivalent design wind load distribution P^* is defined as the most probable load combination at failure (instead of the load pattern which causes a specified maximum response as in the LRC method). This definition allows the consideration of the response, failure mode and structure section based on the maximum failure probability and therefore an objective selection of the response including the consideration of the capacity or strength of the structural elements. The computation of $\mathbf{P}^*$ based on the above definition is shown in the following sections.

3.6.2 Characterization of wind load randomness

The novelty of the presented formulation is based on the approach used to solve the problem of considering simultaneously the wind load as random variables (the maximum mean wind pressure outside the influence of the beam and the peak factor q) and the wind load as a space and time random process defined by the covariance matrix $\mathbf{C}_{p'}$ (e.g. a second moment approximation for non-Gaussian process).To clarify this approach let us consider the following example.

Let us assume that we want to compute the maximum bending moment M_{max} in T_R years (random variable) at a section *i* of the beam of **Errore. L'origine riferimento non è stata trovata.**due to the wind loads. Let us assume that this maximum occurs during a windstorm of duration τ = 1hr. The mean wind pressure during the period τ in the region outside the influence of the beam is w; w is also a random variable: the maximum 1hr mean pressure in T_R years. The wind loads on the beam during the windstorm, **P**(t), are a space and time random process. Therefore, the bending moment M(t) at a section *i* of the beam is also a time random process that can be computed as:

$$M(t)=\mathbf{f}_i^T\mathbf{P}(t)=\mathbf{f}^T\mathbf{P}_0+\mathbf{f}^T\mathbf{P}'(t) \quad (16)$$

Using Eq.14, the maximum bending moment during the windstorm is:

$$M_{max}=\mathbf{f}^T\mathbf{P}_0+q\sigma_M=\mathbf{f}^T\mathbf{p}_0 wA+q\sqrt{\mathbf{f}^T\mathbf{C}_{p'}\mathbf{f}}wA \quad (17)$$

By observation of Eq.17 it can be noticed that there are three sources of randomness in M_{max}: (i) the randomness in the peak factor q (that depends on the mean zero-crossing rate, the skewness and excess kurtosis of the random process and the duration of the storm [122]), (ii) the randomness in the maximum 1hr wind mean pressure in T_R years, w, and (iii) the randomness in the wind load pressure distribution represented by the covariance matrix $\mathbf{C}_{p'}$.

To maintain explicitly the three sources of randomness and for convenience in the reliability analysis that follows, the wind load bending moment, M_w, in the failure equation is written as:

$$M_w=\mathbf{f}^T\mathbf{p}_0 wA+q\mathbf{f}^T\mathbf{p}'wA \quad (18)$$

where **p'** are nominal wind pressure coefficients associated with the covariance matrix $\mathbf{C_{p'}}$, obtained as shown in the following section.

3.6.3 Reliability wind load distribution

Let us assume the following failure equation for each response r_i at the section *i* of the beam of Fig.21 (bending moment, shear, stress, etc):

$$G_i(p') = C_i - r_{Gi} - r_{wi} = C_i - r_{Gi} - \mathbf{f_i^T p_0} wA - \mathbf{f_i^T p'} q_i wA \quad (19)$$

where C_i is the capacity and r_{Gi} is the response due to other loads (gravity loads for example). The design wind pressure coefficients distribution $\mathbf{p'^*}$ is defined as the most probable nominal pressure coefficients combination at failure.

The general methodology to obtain the reliability-based equivalent nominal wind load is to compute β_i solving a minimization problem for each structural member or section and type of failure [125]. Then, the equivalent nominal design wind load coefficients $\mathbf{p'^*}$ are computed for the response r_i with minimum β_i using:

$$\mathbf{p'^*} = \frac{\mathbf{C_{p'} f_i}}{\sqrt{\mathbf{f_i^T C_{p'} f_i}}} \beta_i \alpha_p \quad (20)$$

where α_p is the ratio between the influence on the failure equation of the wind random process divided by the influence of all the random variables.

3.6.4 Stochastic sensibility analysis of Braga stadium roof to wind actions

The Reliability-based wind load distribution was used for the stochastic sensibility analysis of the roof of the Braga Stadium (Fig.7a) under time and spatially random wind loads.

First, wind pressures were obtained from wind tunnel studies on a rigid scaled model. Since the pressure time histories were simultaneously measured at different points, at the upper and the lower sides of the roof panels, the instantaneous pressure fields were available. The roof was divided in n=24 sectors where the wind pressure where measured and averaged at any time t. Therefore, the wind loads on the roof are represented as randomly distributed pressures in n sectors with mean values $\mathbf{p_0}$ and covariance matrix $\mathbf{C_{p'}}$.

Figure 22 shows the mean values of the wind pressure coefficients $\mathbf{p_0}$ (at the left) and the square root of the diagonal of the covariance matrix (standard deviation of p') at the center. A minimum mean value p_0 of about -0.5 is obtained near the border where the wind attacks the roof. A maximum standard deviation $\sigma_{p'}$ of about 0.15 is obtained near that point in the roof corner.

Using the reliability-based method, the spatial distribution of wind loads that drive the structure to fail with most probability is obtained.

Figure 22 on the right shows the $\mathbf{p'^*}$ coefficients at roof failure. A minimum p'^* value about -3.0, concentrated near the border where the wind attack the roof, is obtained. Note that most of the roof has small values of $\mathbf{p'^*}$ showing the high concentration of wind pressure that is expected at failure.

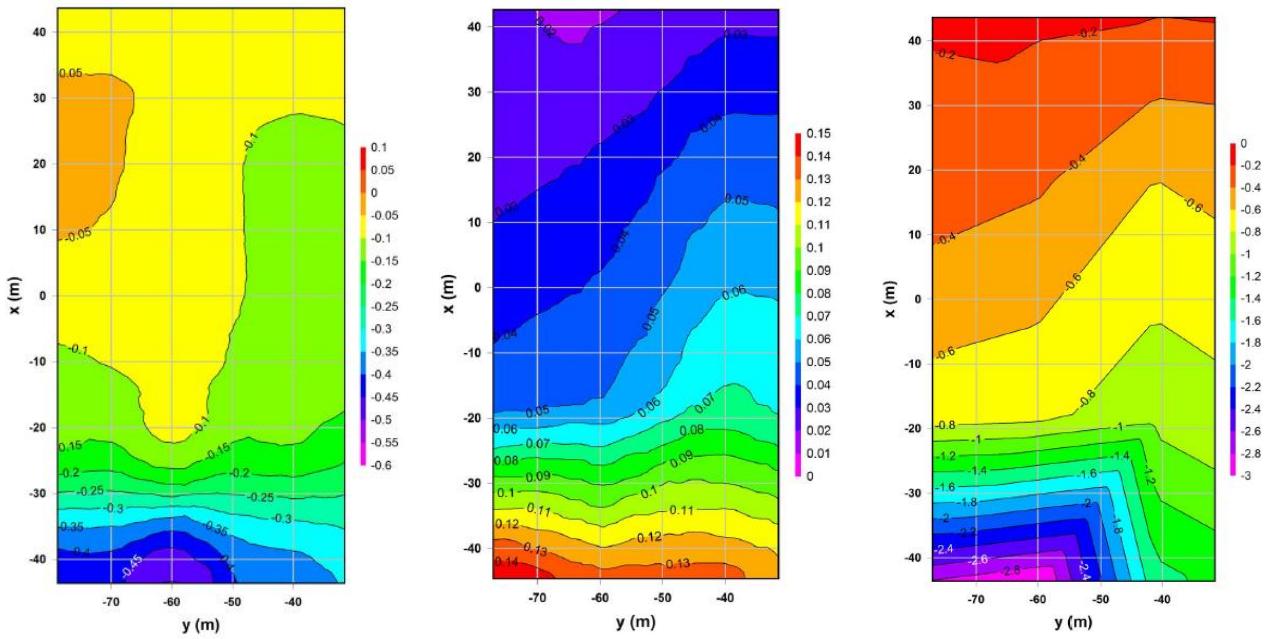

Fig.22 Mean value (a) and standard deviation (b) of wind pressure coefficients and reliability-based wind pressure (c) at left roof

As an improvement with respects to the LRC method, the Reliability-based approach here presented provides the worst spatial wind load distribution associated to the wind variability and the weakness of the roof as well as the minimum safety index β. According to the Reliability-based method, Fig.22 shows the wind pressure coefficients pattern that should be used for designing. This equivalent load distribution is the load pattern that produces the same standard deviation of the bending moment at the point of the roof that will fail with most probability as the experimental data representing the real random process. If the obtained β is too small, the roof should be locally strengthened and the process should be repeated for other sections and type of failures until an acceptable failure probability be achieved.

3.7 Boundary layer wind tunnel testing of wide span enclosures

As already mentioned in the Introduction the effects of the wind on wide span enclosures are not covered by standard codes. For this type of structures Boundary layer wind tunnels are used to define the loads and response of the structure to wind action. .

3.7.1 Wind tunnel description

Boundary layer wind tunnel can reproduce the real turbulent wind blowing to a generic structure. As an example in Fig 23 the wind tunnel of POLIMI is represented, being the largest in Europe for boundary layer wind engineering applications. The wind tunnel has two measure sections as reported in Fig 23: the Section a) is the High Speed - Low Turbulence Section generally used for aerodynamic measures; the Section b) is the Boundary Layer - Higher Turbulence Section, 14m large , 4m tall and 35m long, typically used for Wind Engineering Tests.

Fig 24 shows a picture of the boundary layer test section [130]. It is possible to see the passive turbulence generation devices that are used to obtain the desire turbulent wind profile: it is possible to identify the 9 spires that are installed upstream of the test section, while on the ground there is a distributed roughness. Using the correct combination of spires and floor roughness it is possible to obtain the desired wind profile with the suitable level of turbulence of the site where the structure is placed.

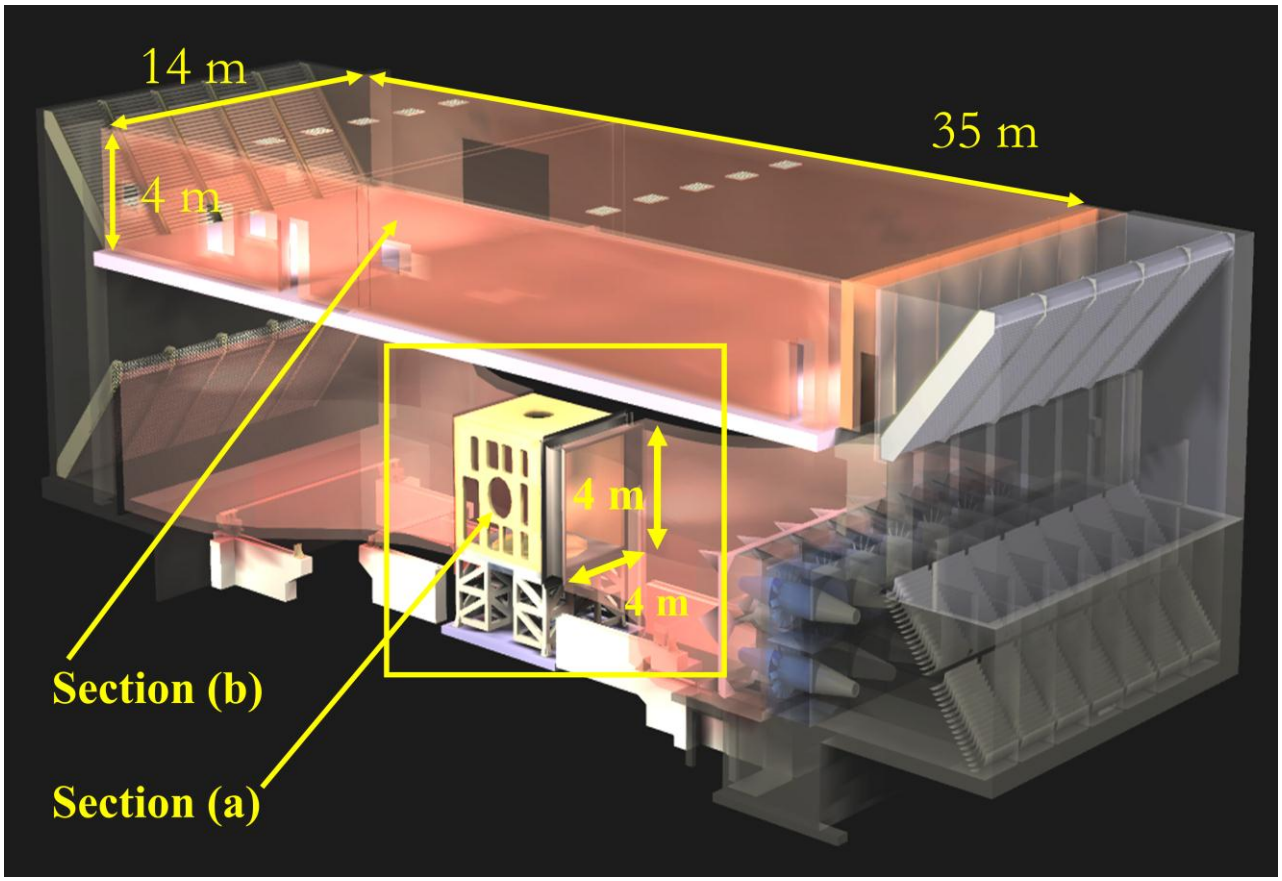

Fig.23. Wind Tunnel of Politecnico di Milano with two measure sections: Section a) High Speed - Low Turbulence Section (aerodynamic measures); Section b) Boundary Layer Higher Turbulence Section (Wind Engineering Tests)

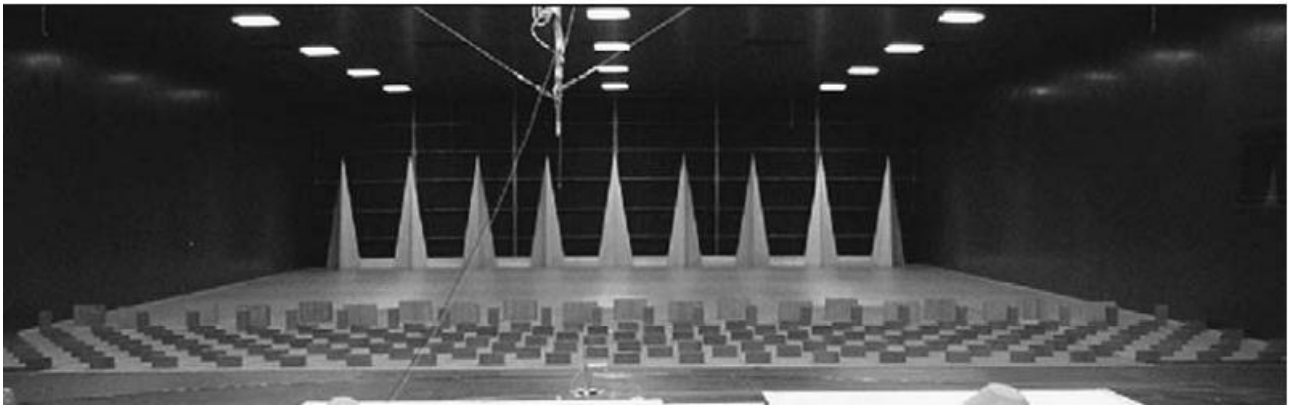

Fig.24. Wind Tunnel of Politecnico di Milano: view of the Boundary Layer Section [130].

In Fig 25 is reported a typical vertical profile of mean wind and along wind turbulence intensity measured in the wind tunnel [130] and it is possible to compare the profiles with the prescriptions of the standards [36] for the target profile type. It is important to obtain a good agreement between the experimental and the prescribed profiles especially in the range where the structure is placed, highlighted by the dash-dotted horizontal line.

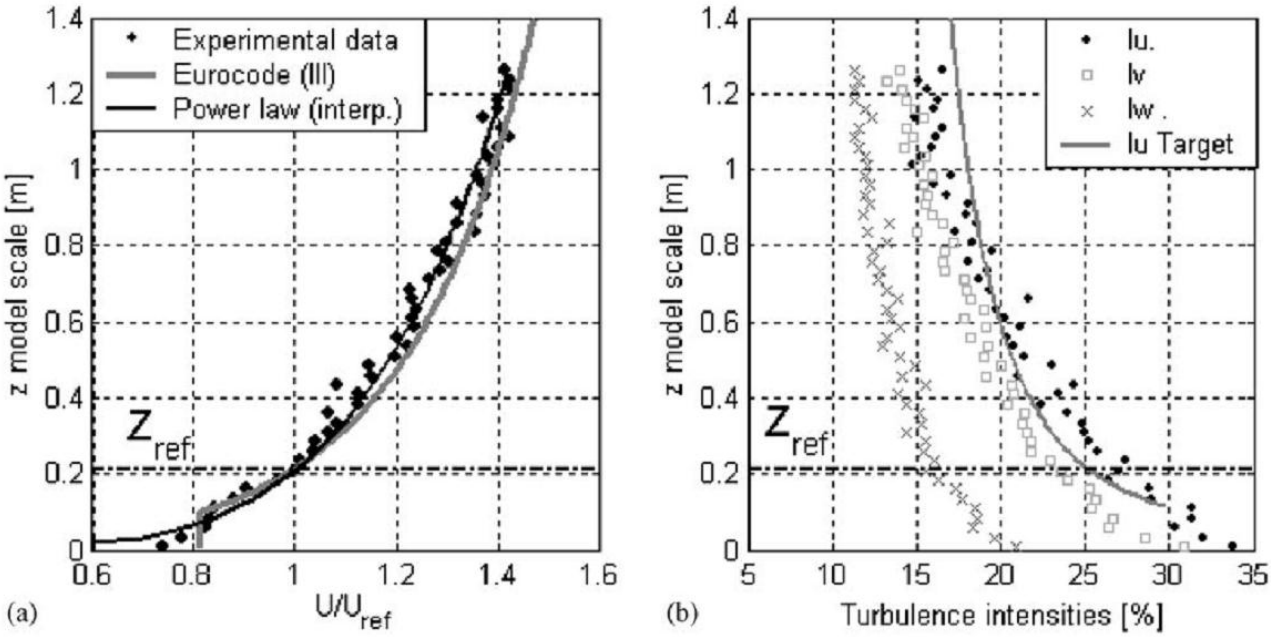

Fig.25. Boundary layer wind tunnel: measured versus target vertical profiles of along wind velocity component: (a) mean wind, (b) turbulent intensity [130]

It is important to correctly reproduce also the dynamic features of the incoming flow, in order to take into account also the turbulent scales that will interact with the structure. The description of the energy content in the flow at different frequencies is described by the Power Spectral Density (PSD), as quoted in Fig. 26, where the PSD of the incoming wind turbulence is reported as measured in the wind tunnel and is compared with the standard prescriptions and the Von Karman formulation of the turbulent wind energy content.

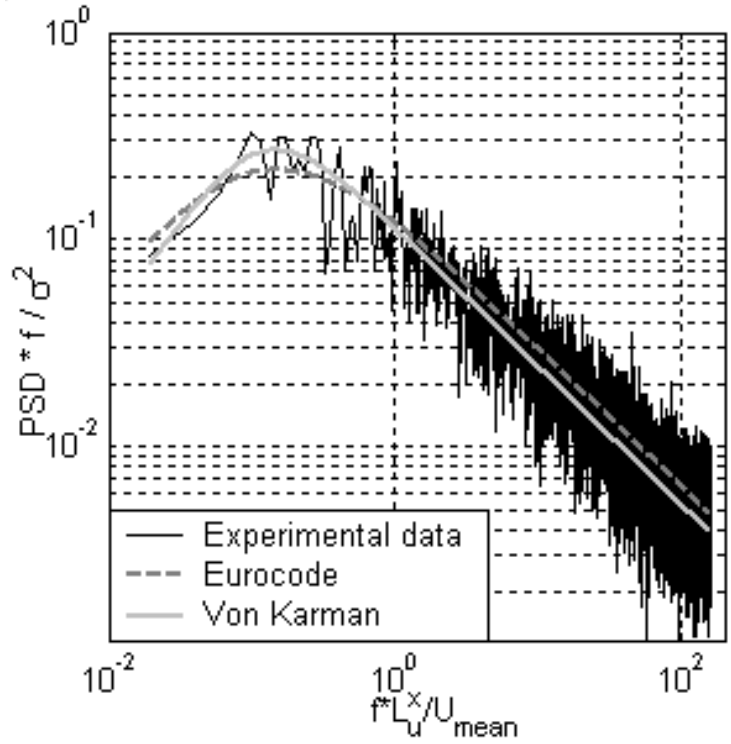

Fig.26. Boundary layer wind tunnel: P.S.D. of measured turbulence compared with standard prescriptions and Von Karman formulation [130]

When reproducing the interaction between the wind incoming turbulence and the building it is important to maintain also the scales of the coherent structures that are impinging the building. The overall parameters representative of that are the Integral Length Scales of turbulence that must therefore be correctly scaled according to the same length scale adopted for the construction.

The typical scales used in the wind tunnel range from 1:70 to 1:250 as a function of the type of structure to be tested. Smaller wind tunnels use a smaller scale, since the flow around the model must not be affected by the walls of the wind tunnel, keeping the blockage as small as possible.

This type of wind tunnel can also be used in smooth flow without reproducing the real turbulence. This type of test is generally used to better reproduce vortex shedding that is sensitive to turbulence and is easily excited with conditions of low level of turbulence, also called smooth flow.

3.7.2 Typology of models

The typology of models to be tested in a wind tunnel can be rigid or aeroelastic.

Rigid Models

Rigid models are used to define the pressure distribution or the overall forces transmitted by the wind, not taking into account aeroelastic effects. As an example in Fig. 27 the New Juventus Stadium in Turin is shown as tested in the wind tunnel is reported [131]. In this case on the roof 500 pressure taps were fitted in order to identify the pressure distribution. The pressure measurements are performed through high speed pressure scanners connected to the pressure taps put on the surface of the structure. This technique allows collecting data at high frequency – of the order of hundreds of Hertz – in order to evaluate the frequencies of the pressure fluctuations that can excite the modes of the roof that must be considered.

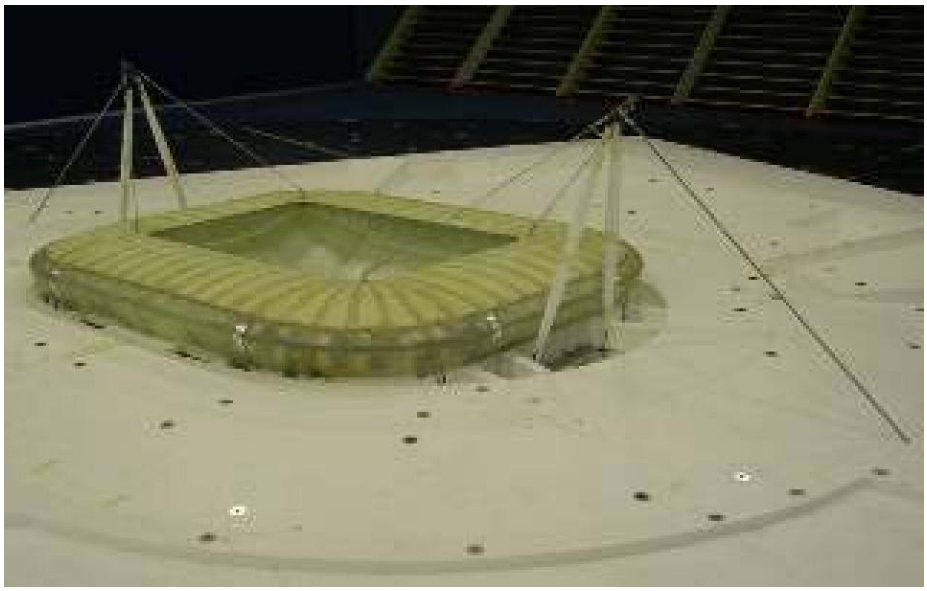

Fig.27. New Juventus Stadium in Turin: example of rigid pressure model [131]

For this reason if the scale of the model is for example 1:100 and the flow velocity in the wind tunnel is of the order of 10-15 m/s, not far from a real wind situation, the sampling frequency should be at least 200 times the frequency of the structure that must be considered.

Decreasing the speed of the flow in the wind tunnel the frequency can be as a consequence reduced but in this case a higher sensitivity is needed in the pressure transducers. As an example in Fig. 28 the pressure average distribution on the New Juventus Stadium in Turin is represented.

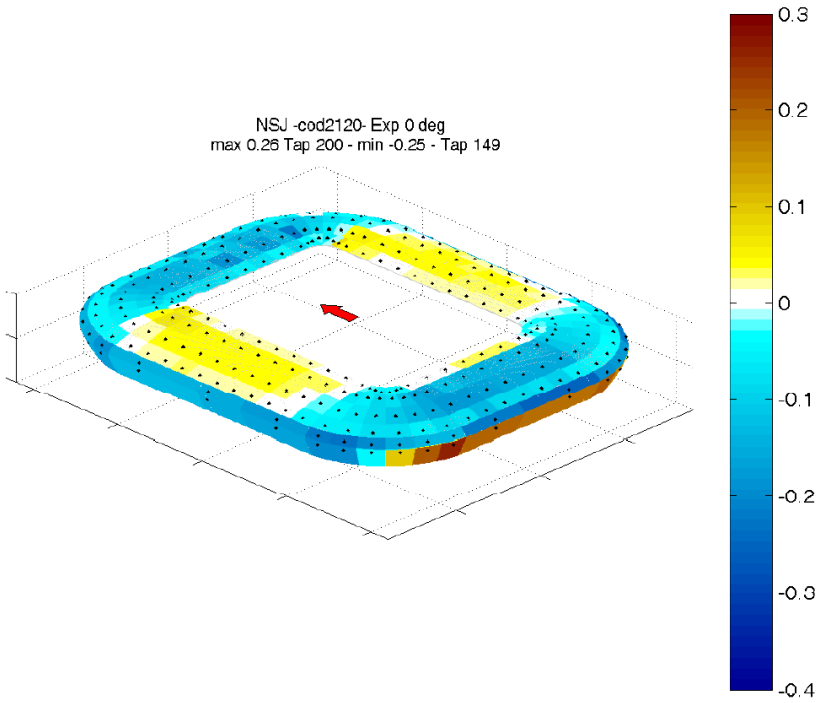

Fig.28. New Juventus Stadium in Turin: average pressure distribution on the roof

In Fig. 29 an other example of rigid model is reported: the Rho exposition. The Logo of the roof of the Rho exposition, which has a typical shape and is reported in Fig. 30, has been analyzed with particular care.

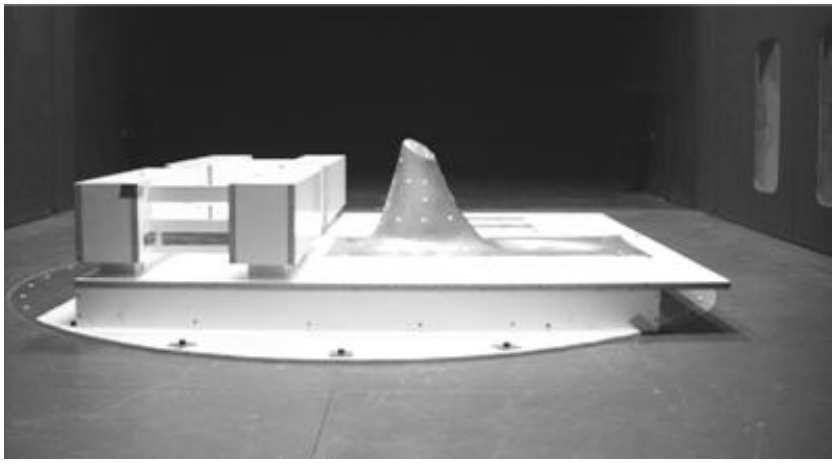

Fig.29. Rho exposition: example of rigid pressure model of the roof allowing for differential pressure reading

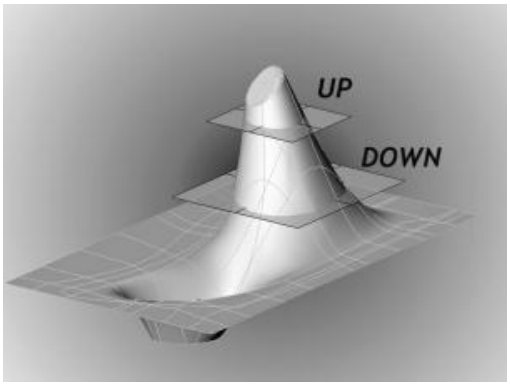

Fig.30. Rho exposition: detail of the Logo rigid pressure model

In Fig. 31 the average pressure distribution along a circular section at a specific elevation is reported. As can be seen the pressure distribution is sensitive to the Reynolds number as always occurs when a curved shape is considered: the location of flow separation changes with the Reynolds number, due to the curvature of the Logo surface.

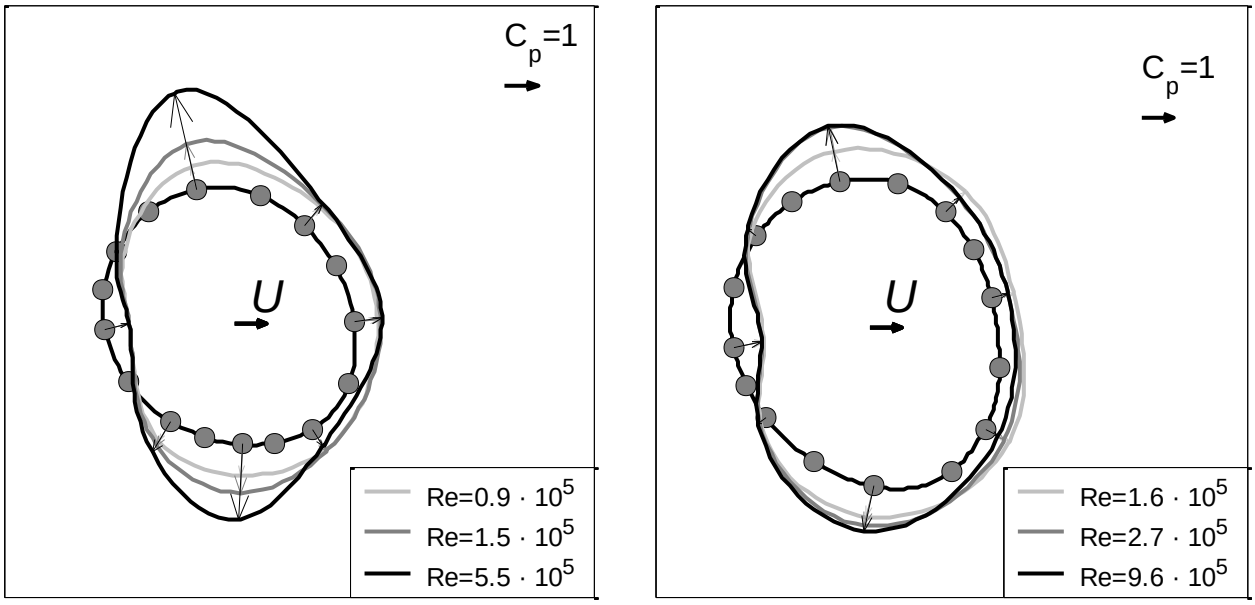

Fig.31. Rho exposition: average pressure distribution on the Logo depending on the Reynolds Number: (left) UP section, (right) DOWN section. The correspondence of the name of the sections is reported in Fig. 30.

In order to try to reproduce the high Reynolds number effect of the real structure in the model in the wind tunnel, the surface roughness of the model has been increased as reported in Fig. 32 and the pressure distribution is much less sensitive the Reynolds Number variations as shown in Fig. 33.

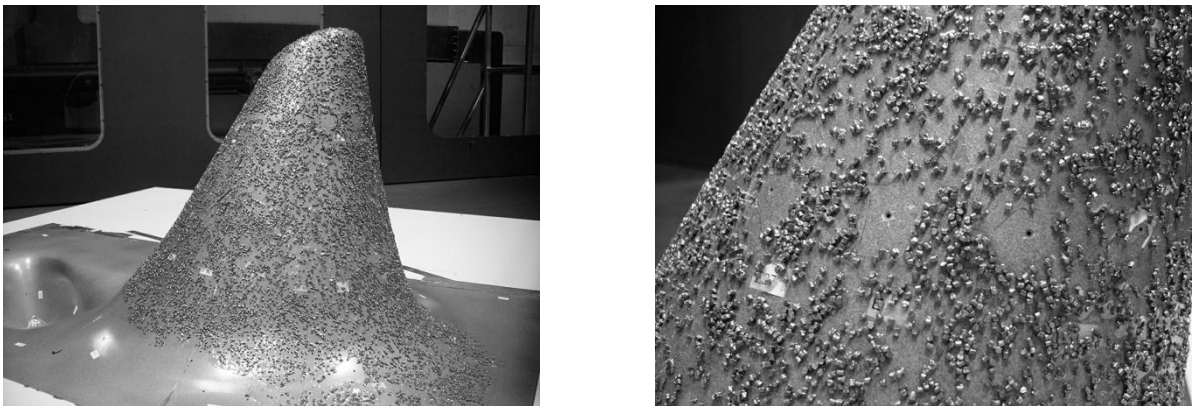

Fig.32. Logo of the Rho exposition: increased surface roughness in rigid model to avoid Reynolds number sensitivity

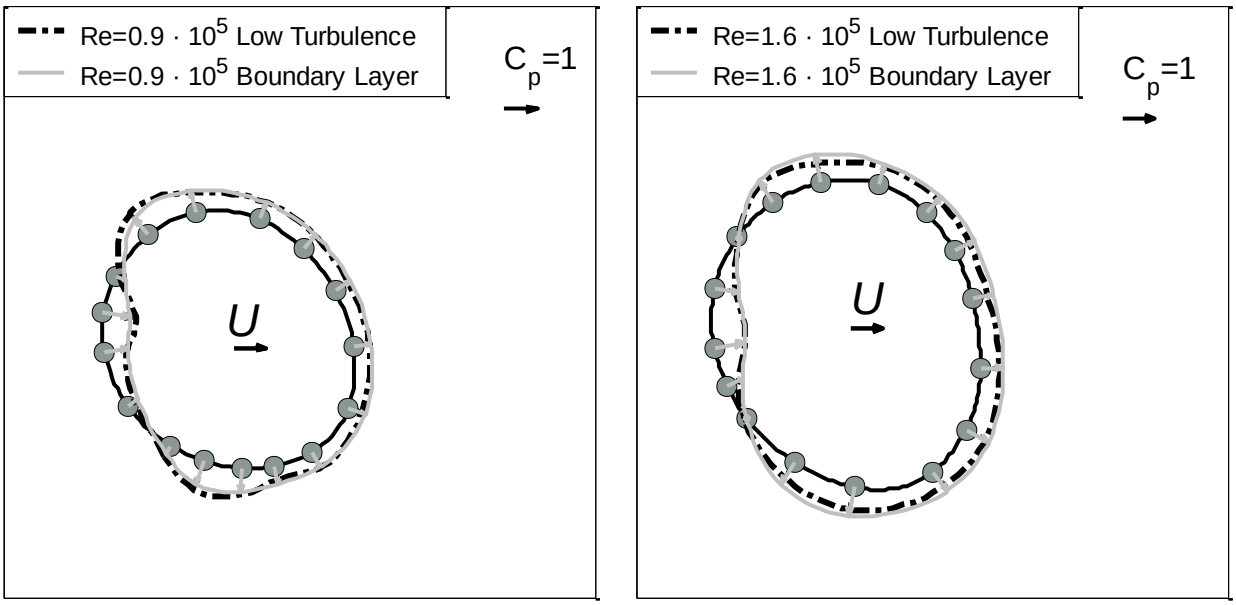

Fig.33. Logo of the Rho exposition: no Reynolds dependence on the average pressure distribution as an effect of increased surface roughness

Aeroelastic Models

Full aeroelastic models of a wide span enclosure are very useful to check all the design procedure, since it is possible to check the actual fluid-structure interaction.

Full aeroelastic models are designed to reproduce the natural frequencies and the mode shapes of the real structure and, using the Froude scaling similitude, the accelerations measured on the model are exactly the accelerations that will be measured in the real structure. Froude scaling implies that the speed used is in the model scale is $\sqrt{\lambda}$ lower than the real velocity being $1/\lambda$ the ratio between the size of the model and the real structure size.

The boundary layer wind tunnel tests shall reproduce in the model scale the real wind velocity profile and the real turbulence of the site as already explained in paragraph 3.7.1, however tests in smooth flow are also used in order to identify possible problems related to flow separation and vortex shedding.

Full aeroelastic models are in condition to reproduce the very complex problem related to the fact

that the pressure distribution deflects the roof and the modified shape of the roof changes the static and dynamic pressure distribution. This type of feed-back due to the aeroelastic interaction is more important as the deformability of the roof is higher. The main issue in this kind of tests is to build an aeroelastic model of the roof in which pressure taps are also installed. The problem is related to the fact that in order to reproduce in the right scale the roof structure, the model should be very light and the installation of pressure taps on the both side of the roof for defining the net pressure load is complex, keeping the damping of the structure at the typical low values of the full scale prototype.

The state of the art of the problem is to identify the static and dynamic pressure distribution on a rigid model and use a FEM approach to identify mode shapes and mode frequencies.

A modal approach can be used and the Lagrangian component for each mode deformed shape can be computed by the pressure measured distribution on a rigid model in a wind tunnel.

The overall motion of the roof can in this way be computed. This approach cannot take into account the aeroelastic interaction but the results can be compared with the motion obtained with an aeroelastic model in order to understand if the aeroelastic effects are important and if the numerical approach is conservative enough.

This type of approach has been applied to the Braga stadium already reported in Chapter **Errore. L'origine riferimento non è stata trovata.** in which the motion of the roof have some effects on the self excited forces induced by the corner of the roof due to flow separation.

CFD techniques can be used to reproduce the flow field and the influence on the pressure distribution due to the deflected shape of the roof but the interaction between structural model and CFD is a very complex task also with the state of the art very fast computers.

Summarizing, rigid models with pressure measurement are very useful to define the static and dynamic loads on wide span enclosures. Analytical tools based on FEM model and modal approach are a useful tool to define the motion and stress on the structure. The final check of this design procedure must be performed on a full aeroelastic model to compare the numerical results of the motion of the roof with the analytical ones.

If the estimated dynamic deflection due to wind interaction is resulting in larger than the allowed maximum displacement or maximum bending of some structural element, a typical solution is the possibility to apply damping devices to the roof in order to control the motion. An example of this situation is represented by the roof of Lingotto in Turin reported in Fig 34 in which is possible to see the cable connecting the roof corner to the building in which dampers are installed. In this case the design of the dampers was made after tests on a full aeroelastic model, see Fig 35 [132]. For this structure after construction some accelerometers were installed on the roof to detect the level of vibration. These values were compared with those obtained in wind tunnel to confirm once again the design of the damping devices.

Fig.34. The "Flying Carpet" roof of Lingotto (Turin): example of application of a damping system [132].

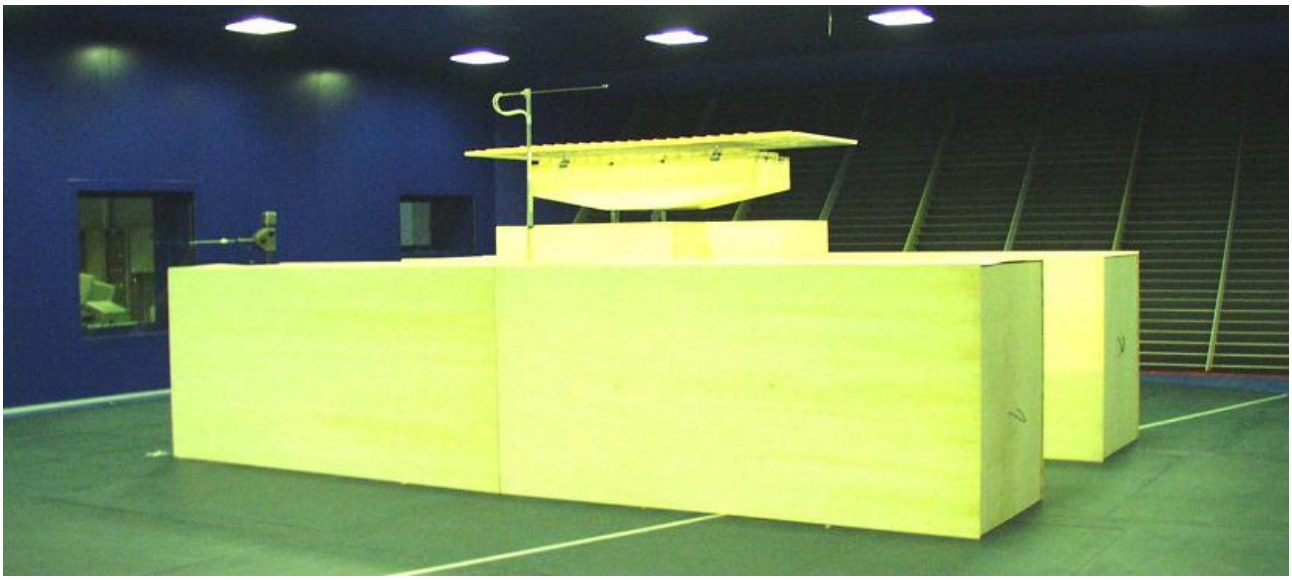

Fig.35. The "Flying Carpet" roof of Lingotto (Turin): full aeroelastic model in Boundary Layer Wind Tunnel [132].

3.8 CFD analyses in the evaluation of the response of wide span enclosures to wind action

Computational Fluid Dynamics (CFD) is a numerical approach to evaluate the wind loads on wide span enclosures. It is considered an approach complementary to the experimental wind tunnel tests for determining the wind actions on structures. This analysis is becoming affordable and reliable in

the last years, but at this purpose the use of High Performance Computing (HPC) resources is requested, since the computational resources required are large due to intrinsic complexity of the fluid-dynamics high Reynolds problems.

CFD offers several advantages if compared with other tools, since it is possible to get the information about the pressure distribution on the entire structure and the description of the flow around the building: it is possible to obtain the local and global loads at the same time. The building geometry can be used for the CFD analysis, and preliminary analysis can be conducted in order to have an estimate of the mean loads acting on the structure.

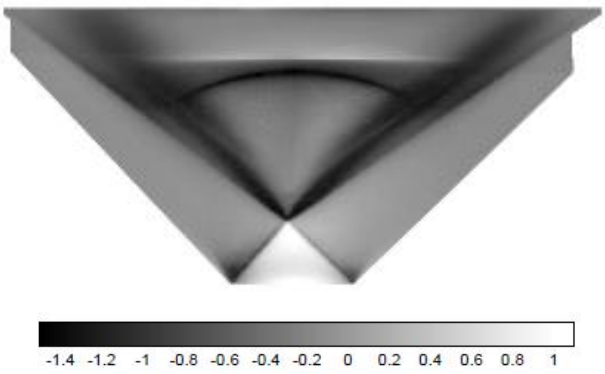

Fig.36. Mean value of pressure coefficients on a non-conventional building [129].

The key point for a correct reproduction of the wind-structure interaction is to adequately model the problem, discretizing with suitable detail the numerical domain and using proper boundary conditions. The discretization is related with the mesh that is used to resolve the Navier-Stokes equations and the relative closure methods: the numerical model has certain mesh requirements that must be combined with the requirements of the problem to be studied; the aim of research institutes as the Architectural Institute of Japan (AIJ) is to give guidelines for the mesh requirements that should be respected in order to assess the wind loads using CFD [126]. As far as it is known by the Authors, AIJ is at present the most active institution making an important effort in writing official recommendations stating the guidelines to be followed by the designers in order to make reliable CFD evaluations of wind effects on structures [127]. The boundary conditions that should be adopted in the definition of the wind loads should be representative of the wind at the building location; therefore the reproduction of the site atmospheric boundary layer is very important for determining the pressure distribution on the structure, as already mentioned for the wind tunnel tests that must take into account the characteristics of the vertical wind profile, in terms of mean and fluctuating components. As an example, in Fig 37 are shown the LES simulated pressure time histories on the surface of a building, compared with the measured one: the unsteadiness of the simulated surface pressure is strongly influenced by the incoming turbulent wind actually simulated by the CFD LES approach. In particular the appearance of the uniform turbulence results show a poor correspondence with the measured data, although being the mean value quite well reproduced. On the other hand, if the actual boundary conditions of the problem are adequately reproduced (boundary layer mean / T.I. / scale length profiles), the simulated transient pressure correctly reproduces the measured quantities also in terms of peak values as well as of mean and variance.

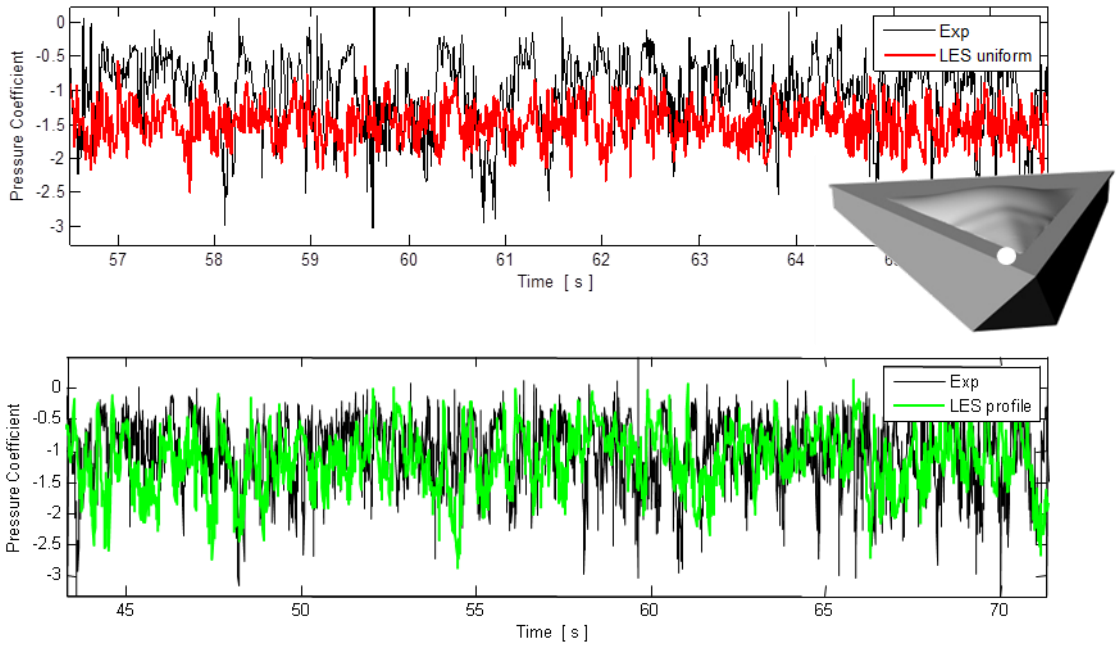

Fig.37. Transient pressure coefficient time histories on a non-conventional building measured and simulated by CFD LES approach (at the white spot) using different turbulent wind profiles with the same turbulence intensity. Black: measured / Red: CFD LES modelling a uniform grid turbulence / Green: CFD LES modelling of the actual wind tunnel boundary layer [128]

Several CFD numerical models can be used, reproducing differently the turbulent fluctuations of the wind: these can be divided in Reynolds Averaged Navier-Stokes (RANS) and Large Eddy Simulations (LES). RANS technique resolves the mean flow field and models the turbulent fluctuations using different approximations: these models are less expensive and less precise and give information about the mean quantities with a reasonable uncertainty. This approach, resolving the steady state flow equations, can be used for a preliminary investigation where the information regarding the peak loads is not necessary and does not requires very high computational resources or calculation time. LES technique allows modeling the flow with the detail provided by the mesh resolution, modeling the smaller flow structures using a sub-grid scale (SGS) model. This model requires large meshes to reproduce with adequate resolution the flow structures and resolves the transient equation of motion. In this case the computational cost is higher, and the use of HPC resources is required but, the results are very valuable, giving accurate results in terms of mean and fluctuating quantities.

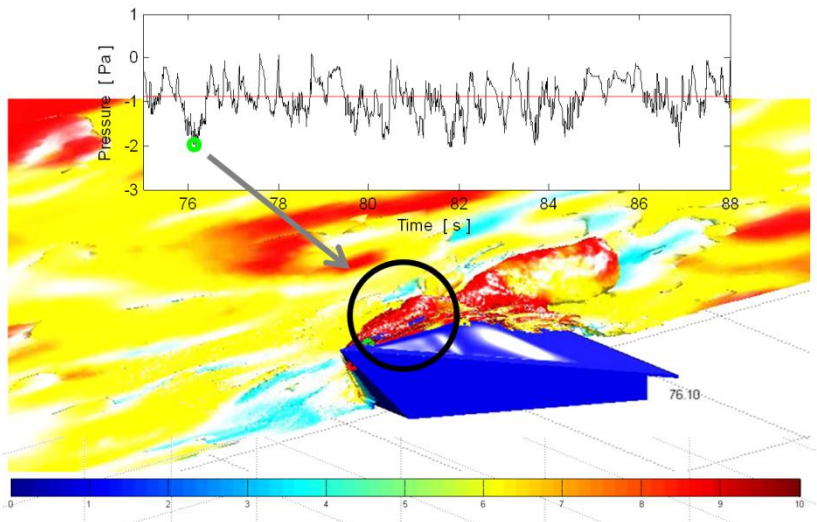

Fig.38. Transient pressure coefficient time history on a non-conventional building and relationship with incoming flow structures [128]

From the above mentioned considerations it is possible to conclude that if a suitable domain discretization is realized it is possible to get reliable mean values by reproducing the correct wind velocity profile, while the peak dimensioning values can be obtained only if the large coherent flow structures are reproduced. The HPC requirements for the transient LES simulations make difficult, at present time, to apply this methodology for design purposes, while it is mainly dedicated to research activity or to very particular and daring structures.

Although with the HPC resources nowadays available is possible to match CFD and wind tunnel tests results with good accuracy in terms of mean and fluctuating quantities, nevertheless the time required for each approach is very similar and at the moment there is no clear advantage in the numerical modeling. It is also very difficult to define the Reynolds number effect on the definition of the wind loads in both approaches. This is a critical point for the wind tunnel tests that are intrinsically performed with Reynolds numbers lower at least of two orders of magnitude than full scale. At the same time in the CFD approach the model approximations have an influence on the largest Reynolds number reached, given the computational resource available. The state of the art at present is focused on the modeling validation of laboratory (wind tunnel) experiments with controlled boundary conditions. There is still at present a lack of information about what are the actual full scale loads in order to determine the accuracy of the full scale modeling. The most critical problem is not just the full scale measure of actual pressures and loads on the façades but mainly the difficulty to define the full scale wind conditions in order to correlate the incoming wind with the loads on the structure.

3.9 Dynamic characterization and vibration mitigation

Dynamic characterization of the prototype structure oriented to model validation and to monitoring of actual response during the lifetime has become important. Since dynamic properties, like modal shapes, frequencies and damping, strongly influence the wind induced response, the dynamic characterization of the prototype is a common task to take into account since the design stage. In addition, the possibility to introduce additional damping in the structure is important, even after a monitoring phase, during the first years of life. By this way, it is possible to obtain a verification of the design assumptions based on theoretical calculations integrated with the tests. Particular attention should be made to large span roofs, for which it is important (i) to have an appropriate exciting system that allows to have significant vibration amplitude (Fig.39) and (ii) to account for non-classical damping, in order to correctly keep the dynamic behaviour [133].

Dynamic characterization of the New Braga Stadium [134] was carried out using two different tests, varying the nature of the excitation. A classical sudden load release has been used to identify the frequency of the first few vibration modes and harmonic excitation of the main vibration modes, to measure the free vibration decay - hence, the inherent damping - (Fig.40).

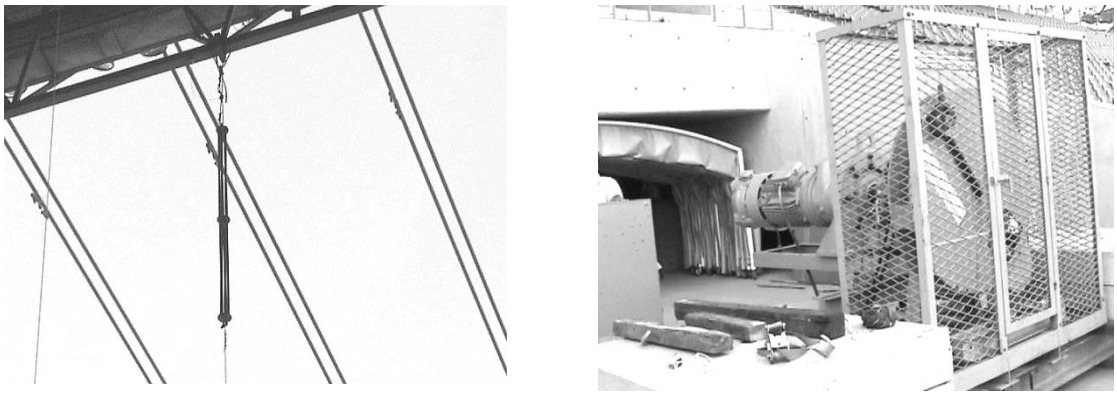

Fig.39 The exciting system used for the dynamic characterization of the New Braga Stadium

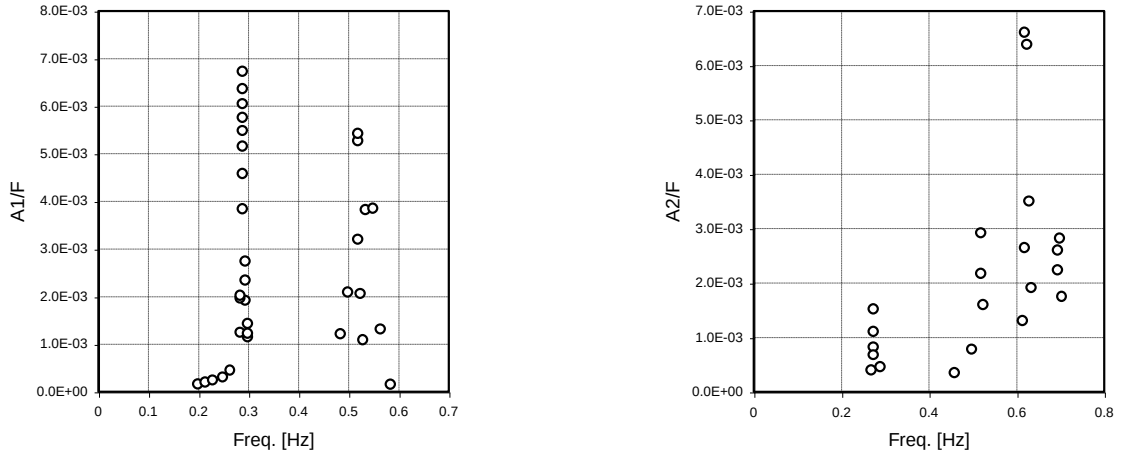

a) b)

Fig.40 Harmonic load: dynamic response ratio vs excitation frequency for a) force in EXC A and b) force in EXC B

By recording the dynamic response of the structure to impulsive and to harmonic loads in terms of accelerations in significant points of the structure, different vibration modes have been identified. The excited and analyzed modes were selected among the vibration that majorly influence the wind response. Results demonstrate that theoretical and experimental mode shapes and frequencies are close to those of the FEM model for anti-symmetric modes and slightly stiffer than the theoretical ones for the symmetric modes and the corresponding frequencies are slightly higher. Modal damping ratios were found to be about 3‰ for almost all the excited modes, especially for the major responsible of the wind induced resonant response that is the most flexible mode.

Tests carried out at Politecnico di Milano on an aeroelastic model of the Braga Stadium [12] in both laminar flow and turbulent flow, revealed that damping devices are necessary to obtain plausible values for amplitudes of vibration. Linear viscous dampers were designed to be located at the roof corners and it was observed that for structural damping up to 7-8%, vibrations decrease at 50% and the amplitude of the torsional frequency is reduced by a factor of three. Nevertheless, the implementation of such dampers was demanded in a second stage, after a monitoring phase oriented to check the actual behavior of the structure, under the natural wind excitation. To evaluate the main property of such a damping system, an estimation of the added damping ratio was carried out through complex eigenvalue analyses [13]. Different time history analyses of the structure subjected to the pressure field measured in the wind tunnel were taken into account to evaluate the behavior

of the damping system and the maximum force produced by the dampers; results in case of undamped structure and with external dampers are provided in Tab.3 for the vertical displacements at the most significant points.

	ξ_i=1% - C=0 daN s/m				ξ_i=1% - C=15000 daN s/m				
	min [cm]	*max* [cm]	μ [cm]	σ [cm]	*min* [cm]	*max* [cm]	μ [cm]	σ [cm]	$V_{max,damp}$ [m/s]
A	-34	+32	+2	10,6	-11	+14	+2	3,8	≈0,27
B	-46	+39	-6	11,1	-24	+10	-6	4,9	≈0,37
E	-35	+48	+8	16,4	-13	+31	+8	6,0	≈0,41
F	-60	+26	-15	16,2	-38	+3	-15	6,8	≈0,34

Tab.3 Comparison of structural responses in terms of vertical displacements in absence and with external dampers

Of note that oscillation amplitudes can be substantially reduced using viscous dampers with a damping coefficient of 15000 daN·s/m, as shown by standard deviations.

REFERENCES

[1] M. Majowiecki, Osservazioni su Indagini Teoriche e Controlli Sperimentali Condotti su Coperture Leggere di Grandi Dimensioni, Official records of the 1° Convegno Nazionale di Ingegneria del Vento, Florence, October 1990

[2] B.J. Vickery, M. Majowiecki, Wind induced response of a cable supported stadium roof, Journal of Wind Engineering and Industrial Aerodynamics, 1992, pp. 1447-1458

[3] M. Majowiecki, Experimental and Reliability Analyses in the Field of Wide Span Steel Structures, Official records of the 4th National Conference on Steel Structures, Patras, Greece, May 24 – 25, 2002

[4] R.E. Melchers, Structural Reliability, Elley Horwood Ltd, 1987

[5] M. Majowiecki, Large span roofs, Proc. of Research Project named "Lifetime performance, innovation and design criteria for structures and infrastructures, against wind actions and other natural events (PERBACCO)". Coord. C. Borri. - Firenze, Giugno 2006

[6] V. Denoël, R. Maquoi, The concept of numerical admittance, Journal of Archives of Applied Mechanics, (in press):10.1007/s00419–012–0686–5, 2012

[7] M. Majowiecki, Experimental Vibration Analysis in Assessment and Design of lightweight Structures, Proc of Int. Conf. "Experimental Vibration Analysis for Civil Engineering Structures" (EVACES), Varenna, Italy, October 2011

[8] A. Flaga, Quasy-Steady Theory of Slender Structures, FSB 151, Sonderforschungsbereich Tragwerksdynamik, Wissenschaftlichte Mitteihungen, Ruhr-Universität Bochum, Berichte Nr 25, 1994

[9] M. Majowiecki, Observations on theretical and experimental investigations on lightweight wide span coverings, International Association for Wind Engeneering, AINV, 1990

[10] B.J. Vickery, Wind loads on the Olympic Stadium – Orthogonal decomposition and dynamic (resonant) effects; BLWT-SS28A, 1993

[11] N. Blaise and V. Denoël. Optimal Processing of Wind Tunnel Measurements in View of Stochastic Structural Design of Large Flexible Structures. Wind Tunnels and Experimental Fluid Dynamic Research. Edited by J. C. Lerner and U. Boldes, InTech, ISBN 978-953- 307-623-2, 2011.

[12] M. Majowiecki, N. Cosentino, Dynamic Aspects of the New Braga Stadium Large Span Roof, Proc. of IASS Symposium 2007, Venice December 3-6

[13] N. Cosentino, M. Majowiecki, Analysis and mitigation of the wind induced response of large span suspended roofs: the case of the new Braga Stadium, Atti dell'8° Convegno Nazionale di Ingegneria del Vento - IN-VENTO-2004, Reggio Calabria, Giugno

[14] B.J. Vickery, Wind loads on the Olympic Stadium: Orthogonal Decomposition and Dynamic (Resonant) Effects, Report BLWT-SS28A, 1993

[15] B.J. Vickery, P.N. Georgiou, A simplified approach to the determination of the influence of internal pressures on the dynamics of large span roofs, Journal of Wind Engineering & Industrial Aerodynamics vol. 38 issue 2-3 July - August, 1991. p. 357-369

[16] B.J. Vickery, R. Basu, Simplified approaches to the evaluation of the across-wind response of chimneys, Journal of Wind Engineering & Industrial Aerodynamics, vol. 14 issue 1-3 December, 1983. p. 153-166

[17] M. Lazzari, R.V. Vitaliani, M. Majowiecki, A.V. Saetta, Dynamic behavior of a tensegrity system subjected to follower wind loading, Computers and Structures 81 2199-2217, 2003

[18] M. Majowiecki, Stadia Roof Structures: design assisted by testing, Official records of the Tensinet Symposium, Designing Tensile Structures, Bruxelles, Belgium, September 19 – 20, 2003

[19] M. Lazzari, M. Majowiecki, R.V. Vitaliani, A.V. Saetta, Nonlinear F.E. Analyses of Montreal Olympic Stadium Roof Under Natural Loading Conditions, Engeneering Structures, Volume 31, Issue 1, January 2009, Pages 16-31

[20] S. Giangreco, S. Geller, M. Krafczyk, V. Sepe, Validation of a lattice Boltzmann Model for Snow Transport and Deposition by Wind, Atti dell'11° Convegno Nazionale di Ingegneria del Vento - IN-VENTO-2010, Spoleto, 30 Giugno – 3 Luglio

[21] W.H. Melbourne, J.C.K. Cheung, Reducing the wind loading on large cantilevered roofs, J. Wind Eng. Ind. Aerodyn, 28, 401–410, 1988

[22] W.H. Melbourne, The response of large roofs to wind action, J. Wind Eng. Ind. Aerodyn, 54/55, 325–335, 1995

[23] G.P. Killen, C.W. Letchford, A parametric study of wind loads on grandstand roofs, Engineering Structures 23, 725–735, 2001

[24] C.W. Letchford, G.P. Killen, Equivalent static wind loads for cantilevered grandstand roofs, Engineering Structures 24, 207–217, 2002

[25] Australian/New Zealand Standard, Structural design actions – Part 2: Wind Actions, AS/NZS 1170,2.2011

[26] H. Kawai, R. Yoshie, R. Wei, M. Shimura, Wind-induced response of a large cantilevered roof. J. Wind Eng., Ind. Aerodyn, 83, 263–275, 1999

[27] Indian Standard, Indian standard code of practice for design loads (other than earthquake) for buildings and structures - IS:875 - part 3 (wind loads), Bureau of Indian Standards, New Delhi, India, Sixth Reprint, 1998

[28] A.G. Davenport, Gust loading factors, Proceedings of the American Society of Civil Engineers, Journal of Structural Division, 93(3):11–34, 1967

[29] B.J. Vickery, On the reliability of gust loading factors, proceedings of the Technical Meet Concerning Wind Loads on Buildings and Structures, National Bureau of Standards, Washington, pages 93–104, 1970

[30] E. Simiu, Gust factors and alongwind pressure correlations, Journal of the Structural Division-Asce, 99(ST4):773–783, 1973

[31] J.D. Holmes, Wind Loading on Structures, SponPress, London, 2nd edition edition, 2007

[32] J. Vellozzi, E. Cohen, Gust response factors, J. STRUCT. ENGNG, (ASCE), 97(6): 1295–1313, 1968

[33] G. Solari, Gust buffeting, Peak wind velocity and equivalent pressure, Journal of structural engineering New York, N.Y., 119(2):365–382, 1993

[34] G. Solari, Gust buffeting, Dynamic alongwing response, Journal of structural engineering New York, N.Y., 119(2):383–398, 1993

[35] J.D. Holmes, Along-wind response of lattice towers: part i - derivation of expressions for gust

response factors, Engineering Structures, 16(4):287–292, 1994

[36] E. Simiu R. Scanlan, Wind Effects On Structures, John Wiley and Sons, 3rd edition, 1996

[37] Eurocode 1, Actions on structures — general actions —part 1-4: Wind actions, 2005

[38] G. Solari, A. Kareem, On the formulation of asce7-95 gust effect factor, Journal of Wind Engineering and Industrial Aerodynamics, 77-78:673–684, 1998

[39] International Standards Organization, ISO 4354 - Wind actions on structures, 2009

[40] Y. Zhou, T. Kijewski, A. Kareem, Along-wind load effects on tall buildings: Comparative study of major international codes and standards, Journal of Structural Engineering, 128 (6):788–796, 2002

[41] Y. Zhou, M. Gu, H. Xiang, Alongwind static equivalent wind loads and responses of tall buildings, part i: Unfavorable distributions of static equivalent wind loads, Journal of Wind Engineering and Industrial Aerodynamics, 79(1-2):135–150, 1999

[42] Y. Tamura, K. Fujii, H. Ueda, Design wind loads for beams supporting flat roofs, Journal of Wind Engineering and Industrial Aerodynamics, 43(1-3):1841–1852, 1992

[43] G.Q. Huang, X. Z. Chen, Wind load effects and equivalent static wind loads of tall buildings based on synchronous pressure measurements, Engineering Structures, 29(10): 2641–2653, 2007

[44] G. Piccardo, G. Solari, 3-d gust effect factor for slender vertical structures, Probabilistic Engineering Mechanics, 17(2):143–155, 2002

[45] A. Kareem, Y. Zhou, Gust loading factor - past, present and future, Journal of Wind Engineering and Industrial Aerodynamics, 91(12-15):1301–1328, 2003

[46] D.W. Seo, L. Caracoglia, Derivation of equivalent gust effect factors for wind loading on low-rise buildings through database-assisted-design approach, Engineering Structures, 32(1):328–336, 2010

[47] Y. Uematsu, M. Yamada, A. Karasu, Design wind loads for structural frames of flat long-span roofs: Gust loading factor for the beams supporting roofs, Journal of Wind Engineering and Industrial Aerodynamics, 66(1):35–50, 1997

[48] Y. Uematsu, M. Yamada, A. Sasaki, Wind-induced dynamic response and resultant load estimation for a flat long-span roof, Journal of Wind Engineering and Industrial Aerodynamics, 65(1-3):155–166, 1996

[49] Y. Uematsu, K. Watanabe, A. Sasaki, M. Yamada, T. Hongo, Wind-induced dynamic response and resultant load estimation of a circular flat roof, Journal of Wind Engineering and Industrial Aerodynamics, 83:251–261, 1999

[50] J.D. Holmes, R. J. Best, An approach to the determination of wind load effects on lowrise buildings, Journal of Wind Engineering and Industrial Aerodynamics, 7(3):273–287, 1981

[51] T. Stathopoulos, Wind loads on low-rise buildings: a review of the state of the art. Engineering Structures, 6(2):119–135, 1984

[52] J.D. Holmes, Distribution of peak wind loads on a low-rise building, Journal Of Wind Engineering and Industrial Aerodynamics, 29(1-3):59–67, 1988

[53] M. Kasperski, Extreme wind load distributions for linear and nonlinear design, Engineering Structures, 14(1):27–34, 1992

[54] M. Kasperski, H. J. Niemann, The l.r.c. (load-response-correlation) - method a general method of estimating unfavourable wind load distributions for linear and non-linear structural behavior, Journal of Wind Engineering and Industrial Aerodynamics, 43(1-3): 1753–1763, 1992

[55] Y. Uematsu, T. Moteki, T. Hongo, Model of wind pressure field on circular flat roofs and its application to load estimation, Journal of Wind Engineering and Industrial Aerodynamics, 96 (6-7):1003–1014, 2008

[56] M. Kasperski, Incorporation of the lrc-method into codified wind load distributions, In Proceedings of The Seventh Asia-Pacific Conference on Wind Engineering, 2009

[57] A.G. Davenport, The representation of the dynamic effects of turbulent wind by equivalent static wind loads, Proceedings of the Int. Engineering Symposium on Structural Steel, pages 1–13, 1985

[58] J.D. Holmes, Along-wind response of lattice towers – iii, effective load distributions, Engineering Structures, 18(7):489–494, 1996

[59] J. Holmes, G. Wood, The determination of structural wind loads for the roofs of several venues for the 2000 olympics, volume 109, 2001

[60] Y. Zhou, A. Kareem, M. Gu, Equivalent static buffeting loads on structures, Journal of Structural Engineering-Asce, 126(8):989–992, 2000

[61] X. Z. Chen, A. Kareem, Equivalent static wind loads for buffeting response of bridges, Journal of Structural Engineering-Asce, 127(12):1467–1475, 2001

[62] J.D. Holmes, Effective static load distributions in wind engineering, Journal of Wind Engineering and Industrial Aerodynamics, 90(2):91–109, 2002

[63] M.P. Repetto, G. Solari, Equivalent static wind actions on vertical structures, Journal of Wind Engineering and Industrial Aerodynamics, 92(5):335–357, 2004

[64] Y.Q. Li, Y. Tamura, Equivalent static wind load estimation in wind-resistant design of single-layer reticulated shells, Wind and Structures, An International Journal, 8(6): 443–454, 2005

[65] J.Y. Fu, Z.N. Xie, Q. S. Li, Equivalent static wind loads on long-span roof structures, Journal of Structural Engineering-Asce, 134(7):1115–1128, 2008

[66] N. Blaise and V. Denoël, Principal static wind loads, Journal of Wind Engineering and Industrial Aerodynamics, 113:29–39, 2013

[67] I. Jolliffe, Principal Component Analysis, Encyclopedia of Statistics in Behavioral Science, John Wiley & Sons, Ltd, 2005

[68] A. Katsumura, Y. Tamura, O. Nakamura, Universal wind load distribution simultaneously reproducing largest load effects in all subject members on large-span cantilevered roof, Journal of Wind Engineering and Industrial Aerodynamics, 95(9-11):1145–1165, 2007

[69] R.J. Best, J. D. Holmes, Use of eigenvalues in the covariance integration method for determination of wind load effects, Journal of Wind Engineering and Industrial Aerodynamics, 13(1-3):359–370, 1983

[70] B. Bienkiewicz, Y. Tamura, H J. Ham, H. Ueda, K. Hibi, Proper orthogonal decomposition and reconstruction of multichannel roof pressure, Journal of Wind Engineering and Industrial Aerodynamics, 54:369–381, 1995

[71] G. Solari, L. Carassale, F. Tubino, Proper orthogonal decomposition in wind engineering, part 1: A state-of-the-art and some prospects, Wind And Structures, 10(2):153–176, 2007

[72] X. Chen, N. Zhou, Equivalent static wind loads on low-rise buildings based on full-scale pressure measurements, Engineering Structures, 29(10):2563–2575, 2007

[73] Y.Q. Li, L. Wang, Y. Tamura, Z.-Y. Shen, Universal equivalent static wind load estimation for spatial structures based on wind-induced envelope responses, In Symposium of the International Association for Shell and Spatial Structures (50th. Valencia), 2009

[74] X. Zhou, M. Gu, G. Li, Application research of constrained least-squares method in computing equivalent static wind loads, In Proceedings of the 13th International Conference on Wind Engineering, 2011

[75] A. Katsumura, Y. Tamura, O. Nakamura, Application of universal equivalent static wind load, Proceedings of the 13th ICWE, Amsterdam, The Netherlands, 2011

[76] A. Fiore, P. Monaco, Pod-based representation of the alongwind equivalent static force for long-span bridges, Wind and Structures, An International Journal, 12(3):239–257, 2009

[77] N. Blaise, L. Hamra, V. Denoël, Principal static wind loads on a large roof structure, In Proceedings of the 12th ANIV conference of wind engineering In Vento, 2012

[78] A. Papoulis, Probability, Random Variables, and Stochastic Processes, McGraw Hill, New York, 1965

[79] J.L. Lumley, The Structure of Inhomogeneous Turbulent Flows, A.M. Yaglom and V.I. Tatarski, editors, Atmospheric turbulence and radio propagation, pages 166–178, Nauka, Moscow, 1967

[80] M. Loeve, Probability theory I, 4th edidtion. Probability theory I, 4th edition, Springer- Verlag, 1977

[81] K.R. Gurley, M.A. Tognarelli, A. Kareem, Analysis and simulation tools for wind engineering, Probabilistic Engineering Mechanics, 12(1):9–31, 1997

[82] L. Carassale, G. Solari, F. Tubino, Proper orthogonal decomposition in wind engineering. part 2: Theoretical aspects and some applications, Wind and Structures, 10(2):177–208, 2007

[83] M. Di Paola, Digital simulation of wind field velocity, Journal of Wind Engineering and Industrial Aerodynamics, 74-76:91–109, 1998

[84] L. Carassale, Pod-based filters for the representation of random loads on structures, Probabilistic Engineering Mechanics, 20(3):263–280, 2005

[85] M. Di Paola, I. Gullo, Digital generation of multivariate wind field processes, Probabilistic Engineering Mechanics, 16(1):1–10, 2001

[86] L. Carassale, G. Solari, Wind modes for structural dynamics: A continuous approach, Probabilistic Engineering Mechanics, 17(2):157–166, 2002

[87] G. Solari, F. Tubino, A turbulence model based on principal components, Probabilistic Engineering Mechanics, 17(4):327–335, 2002

[88] F. Tubino, G. Solari, Double proper orthogonal decomposition for representing and simulating turbulence fields, Journal of Engineering Mechanics-Asce, 131(12):1302–1312, 2005

[89] R.H. Scanlan, N. P. Jones, A form of aerodynamic admittance for use in bridge aeroelastic

analysis, Journal Of Fluids And Structures, 13(7-8):1017–1027, 1999

[90] D. Han, J. Li, Application of proper orthogonal decomposition method in wind field simulation for roof structures, Journal of Engineering Mechanics, 135(8):786–795, 2009

[91] J. Armitt, Eigenvector analysis of pressure fluctuations on the west burton instrumented cooling tower, Central Electricity Research Laboratories (UK), Internal Report RD/LN/11/68, 1968

[92] B. Bienkiewicz, H.J. Ham, Y. Sun, Proper orthogonal decomposition of roof pressure, Journal of Wind Engineering and Industrial Aerodynamics, 50(1-3):193–202, 1993

[93] T.C.E. Ho, A.G. Davenport, D. Surry, Characteristic pressure distribution shapes and load repetitions for the wind loading of low building roof panels, Journal of Wind Engineering and Industrial Aerodynamics, 57(2-3):261–279, 1995

[94] J.D. Holmes, R. Sankaran, K.C.S. Kwok, M.J. Syme, Eigenvector modes of fluctuating pressures on low-rise building models, Journal of Wind Engineering and Industrial Aerodynamics, 71:697–707, 1997

[95] H.L. Van Trees, Detection, estimation and modulation theory, Part 1. New York, N.Y., 1968

[96] P.D. Spanos, Roger Ghanem, Stochastic finite element expansion for random media, Journal of Engineering Mechanics, 115(5):1035–1053, 1989

[97] Y. Tamura, S. Suganuma, H. Kikuchi, K. Hibi, Proper orthogonal decomposition of random wind pressure field, Journal of Fluids and Structures, 13(7-8):1069–1095, 1999

[98] A.G. Davenport, How can we simplify and generalize wind loads, Journal of Wind Engineering and Industrial Aerodynamics, 54:657–669, 1995

[99] B. Bienkiewicz, New tools in wind engineering, Journal of Wind Engineering and Industrial Aerodynamics, 65(1-3):279–300, 1996

[100] C.W. Letchford, R.E. Iverson, J.R. McDonald, The application of the quasi-steady theory to full scale measurements on the texas tech building, Journal of Wind Engineering and Industrial Aerodynamics, 48(1):111–132, 1993

[101] F. Rizzo, P. D'Asdia, M. Lazzari, G. Olivato, Aerodynamic behaviour of hyperbolic paraboloid shaped roofs: Pod and cfd analysis, 2009

[102] H. Liu, W.L. Qu, Q.S. Li, Comparison between wind load by wind tunnel test and in-site measurement of long-span spatial structure, Wind and Structures, An International Journal, 14(4):301–319, 2011

[103] S. Benfratello, G. Muscolino, Filter approach to the stochastic analysis of mdof windexcited structures, Probabilistic Engineering Mechanics, 14(4):311–321, 1999

[104] G. Solari, L. Carassale, Modal transformation tools in structural dynamics and wind engineering, Wind And Structures, 3(4):221–241, 2000

[105] L. Carassale, G. Piccardo, G. Solari, Double modal transformation and wind engineering applications, Journal Of Engineering Mechanics-Asce, 127(5):432–439, 2001

[106] X.Z. Chen, A. Kareem, Coupled dynamic analysis and equivalent static wind loads on buildings with three-dimensional modes, Journal of Structural Engineering-Asce, 131(7): 1071–1082, 2005

[107] F. Tubino, G. Solari, Gust buffeting of long span bridges: Double modal transformation and

effective turbulence, Engineering Structures, 29(8):1698–1707, 2007

[108] N. Blaise, G. Grillaud, V. De Ville de Goyet, V. Denoël, Application of deterministic and stochastic analysis to calculate a stadium with pressure measurements in wind tunnel, In Proceedings of 8th International Conference on Structural Dynamics, Leuven, Belgium, 2011

[109] F.B. Chen, Q.S. Li, J.R. Wu, J.Y. Fu, Wind effects on a long-span beam string roof structure: Wind tunnel test, field measurement and numerical analysis, Journal of Constructional Steel Research, 67(10):1591–1604, 2011

[110] R.W. Clough, J. Penzien, Dynamics of structures. McGraw-Hill, New-York, 2nd edition, 1993

[111] N. Blaise, V. Denoël, Optimal Processing of Wind Tunnel Measurements in View of Stochastic Structural Design of Large Flexible Structures, Wind Tunnels and Experimental Fluid Dynamic Research, edited by J.C. Lerner and U. Boldes, InTech, ISBN 978-953-307-623-2, 2011

[112] C. Borri, M. Majowiecki, P. Spinelli, Wind response of a large tensile structure: The new roof of the olimpic stadium in rome, Journal of Wind Engineering and Industrial Aerodynamics, 42(1-3):1435–1446, 1992

[113] C. Borri, W. Zahlten, Fully simulated nonlinear analysis of large structures subjected to turbulent artificial wind, Mechanics of Structures and Machines, 19(2):213–250, 1991

[114] M. Suzuki, S. Sanada, Y. Hayami, S. Ban, Prediction of wind-induced response of a semi-rigid hanging roof, Journal of Wind Engineering and Industrial Aerodynamics, 72 (1-3):357–366, 1997

[115] G. Augusti, C. Borri, L. Marradi, P. Spinelli, On the time-domain analysis of wind response of structures, Journal of Wind Engineering and Industrial Aerodynamics, 23(C): 449–463, 1986

[116] P. Biagini, C. Borri, M. Majowiecki, M. Orlando, L. Procino, Blwt tests and design loads on the roof of the new olympic stadium in Piraeus, Journal of Wind Engineering and Industrial Aerodynamics, 94(5):293–307, 2006

[117] P. Biagini, C. Borri, L. Facchini, Wind response of large roofs of stadions and arena, Journal of Wind Engineering and Industrial Aerodynamics, 95(9-11):871–887, 2007

[118] N. Blaise, V. Denoël, Stochastic analysis of a stadium roof from deterministic wind tunnel measurements, In Proceedings of 13th International Conference on Wind Engineering, 2011

[119] O. Nakamura, Y. Tamura, K. Miyashita, M. Itoh, A case study of wind pressure and wind-induced vibration of a large span open-type roof, Journal of Wind Engineering and Industrial Aerodynamics, 52(C):237–248, 1994

[120] J. Fu, Z. Xie, Q.S. Li, Equivalent Static Wind Loads on Long-Span Roof Structures, Journal of Structural Engineering, ASCE, Vol. 134, No. 7, 1115-1127, 2008

[121] B. Ellingwood, Reliability Basis of Load and Resistance Factors for Reinforced Concrete Design, National Bureau of Standards Building Science Series 110, National Bureau of Standars, Washington, pag. 94, February 1978

[122] D.K. Kwon, A. Kareem, Peak Factors for Non-Gaussian Load Effects Revisited, Journal of Structural Engineering, ASCE, Vol. 137, 1611-1619, No. 12, December 2011

[123] C. Floris, L.D. Iseppi, The Peak Factor for Gust Loading: A Review and Some New Proposals, Meccanica 33(3): 319-330, 1998

[124] A.G. Davenport, Note on the Distribution of the Largest Value of a Random Functions with Application to Gust Loading, Proceedings, Institution of Civil Engineers, Vol. 28, pp. 187-196, 1964

[125] M. Shinozuka, Basic analysis of structural safety, J. Struct. Engrg., ASCE, 109(3), 721–740, 1983

[126] Tamura T., Nozawa K., Kondo K., (2006). ‘‘AIJ guide for numerical prediction of wind loads on buildings’’ CWE 2006, Yokohama, Japan.

[127] Kondo K., (2012). ‘‘AIJ guideline of CFD techniques for wind load estimation’’ BBAA7 2012, Shanghai, China.

[128] Rocchi D., Schito P., Zasso A., (2011). "Investigation on the relation between incoming wind characteristics and surface pressure distribution", 13th International Conference on Wind Engineering, Amsterdam – The Netherlands.

[129] Zasso A., Rocchi D., Schito P., (2009). "Experimental and numerical study of the flow around a low rise building (CC)", 5th European and African Conference on Wind Engineering, Florence – Italy.

[130] Zasso A., Giappino S., Muggiasca S., (2006). "Wind tunnel study of a cone-like shaped roof: Reynolds number effects", Journal of Wind Engineering and Industrial Aerodynamics, Vol. 94, pp. 431-444.

[131] Diana G., Rocchi D., Sabbioni E., Giappino S., Collina A., (2009), "Wind tunnel tests on the roof of the new Turin Stadium", EACWE5, Florence – Italy

[132] Belloli M., Rocchi D., Zasso A., (2003), "Wind-structure interaction of a large flexible roof: comparison of wind tunnel-numerical results and full scale measurement", ICWE2003, Lubbock (TX) - USA

[133] V. Denoël, On the background and biresonant components of the random response of single degree-of-freedom systems under non-Gaussian random loading, Engineering Structures, Volume 33, Issue 8, Pages 2271-2283, August 2011

[134] N. Cosentino, M. Majowiecki, M. Marini, Dynamic characterization of the New Braga Stadium large span suspension roof, Experimental Vibration Analysis for Civil Engineering Structures – EVACES 2005, Bordeaux, October 2005